UNIVERSIDADE FEDERAL DE SANTA MARIA
CENTRO DE CIÊNCIAS RURAIS
PROGRAMA DE PÓS-GRADUAÇÃO EM MEDICINA VETERINÁRIA

ECOGRAFIA MODO-B E DOPPLER NA AVALIAÇÃO DAS ARTÉRIAS EPIGÁSTRICAS SUPERFICIAIS NO NEOPLASMA MAMÁRIO CANINO

Carlos Eduardo Bortolini

Santa Maria, RS, Brasil
2018

Carlos Eduardo Bortolini

ECOGRAFIA MODO-B E DOPPLER NA AVALIAÇÃO DAS ARTÉRIAS EPIGÁSTRICAS SUPERFICIAIS NO NEOPLASMA MAMÁRIO CANINO

Tese apresentada ao Programa de Pós-Graduação em Medicina Veterinária, da Universidade Federal de Santa Maria (UFSM, RS), como requisito parcial para obtenção do título de **Doutor em Medicina Veterinária**

Orientadora: Prof.ª Cinthia Melazzo de Andrade

Santa Maria, RS, Brasil
2018

Carlos Eduardo Bortolini

ECOGRAFIA MODO-B E DOPPLER NA AVALIAÇÃO DAS ARTÉRIAS EPIGÁSTRICAS SUPERFICIAIS NO NEOPLASMA MAMÁRIO CANINO

Tese apresentada ao Programa de Pós-Graduação em Medicina Veterinária, da Universidade Federal de Santa Maria (UFSM, RS), como requisito parcial para obtenção do título de **Doutor em Medicina Veterinária**

Aprovado em 17 de agosto de 2018:

_____

Cinthia Melazzo de Andrade, Dr. (UFSM)
(Presidente/Orientador)

_____

Márcio Machado Costa, Dr. (UPF)
(Coorientador)

_____

Cibele Figueira Carvalho, Dr. (NAUS) - Videoconferência

_____

Fabíola Dalmolin, Dr. (UFFS)

_____

Ricardo Pozzobon, Dr. (UFSM)

_____

Saulo Tadeu Lemos Pinto Filho, Dr. (UFSM)

Santa Maria, RS
2018

RESUMO

ECOGRAFIA MODO-B E DOPPLER NA AVALIAÇÃO DAS ARTÉRIAS EPIGÁSTRICAS SUPERFICIAIS NO NEOPLASMA MAMÁRIO CANINO

AUTOR: Carlos Eduardo Bortolini
ORIENTADORA: Cinthia Melazzo de Andrade

Os objetivos deste estudo foram avaliar a hemodinâmica das artérias epigástricas superficiais cranial e caudal ao Doppler ultrassonográfico, identificar os atributos ultrassonográficos vasculares e da textura tumoral, mensurar o fator de crescimento endotelial vascular e interleucina-8 de pacientes caninos com carcinomas mamários canino, bem como predizer o comportamento biológico do carcinoma mamário a partir das variações hemodinâmicas das artérias epigástricas superficiais em estádios oncológicos iniciais. Para tal, foram avaliados ao Doppler as velocidades de fluxo e o índice de resistividade das artérias epigástricas superficiais cranial e caudal de 63 cadelas. O grupo tumor mamário foi composto por 43 fêmeas com diagnóstico histopatológico de carcinoma mamário e o grupo controle por 20 fêmeas hígidas. A dinâmica vascular foi significativamente diferente entre os grupos, sendo que o número de lesões influenciou nas velocidades, bem como a ecotextura e a apresentação e distribuição dos vasos contribuíram para o índice de resistividade dentro do grupo carcinoma mamário. Também, 50 cadelas foram divididas em dois grupos (13 fêmeas hígidas e 37 com carcinoma mamário), para avaliar a aplicação clínica da mensuração sérica do fator de crescimento endotelial vascular, da interleucina-8 e do estradiol em conjunto com os achados ultrassonográficos do tumor maligno, que demonstrou influência significativa da ecotextura na dosagem da interleucina-8 e a correlação positiva entre as velocidades de fluxo dos vasos tumorais e a mensuração do fator de crescimento endotelial vascular. Esses achados indicam uma relação entre o ambiente tumoral e a expressão da interleucina-8, bem como da dinâmica de fluxo sobre o fator de crescimento endotelial vascular. Ainda, 142 nódulos ou massas mamárias foram avaliados pelo exame ultrassonográfico, para identificar atributos da dinâmica de fluxo tumoral e diferenciar tumores mamários benignos e malignos. A biodinâmica dos vasos internos foi significativamente diferente entre benignos e malignos, sendo que as velocidades sistólica e diastólica sofreram variações a partir do tamanho e da ecotextura tumoral. Dessa forma, a avalição conjunta do tamanho, da ecotextura e da velocidade de fluxo dos vasos internos tumorais, podem ser considerados parâmetros promissores na diferenciação entre tumores mamários benignos e malignos. Desse modo, o presente estudo apresenta uma importante aplicação da ultrassonografia na oncologia veterinária, demonstrando o impacto hemodinâmico nas artérias epigástricas superficiais cranial e caudal ao Doppler ultrassonográfico no carcinoma mamário canino, particularmente quando associado ao tamanho, ecotextura e apresentação e distribuição dos vasos tumorais. Esses achados confirmam que os fatores mecânicos tumorais interferem na hemodinâmica das epigástricas superficiais. Diante dos resultados, sugere-se a avaliação das artérias que irrigam a cadeia mamária acometida, juntamente com outros fatores já relacionados como preditivos de malignidade tumoral, como o tamanho do tumor, a ecotextura heterogênea do estroma tumoral, a apresentação heterogenia e distribuição complexa da vascularização tumoral e a mensuração sérica do fator de crescimento endotelial vascular e da interleucina-8.

Palavras-chave: Vascularização. Ecotextura heterogênea. Velocidade de fluxo. Índice de Resitividade.

ABSTRACT

B-MODE AND DOPPLER ECOGRAPHY IN THE EVALUATION OF SUPERFICIAL EPIGASTRIC ARTERIES IN CANINE MAMMARY NEOPLASM

AUTHOR: Carlos Eduardo Bortolini
ADVISER: Cinthia Melazzo de Andrade

The objectives of this study were to evaluate the hemodynamics of cranial and caudal superficial epigastric arteries on Doppler ultrasound, identify the ultrasound characteristics of the vessels and of the tumor texture, measure the levels of vascular endothelial growth factor (VEGF) and interleukin-8 of canine patients with mammary carcinomas, and predict the biological behavior of mammary carcinoma based on the hemodynamic variations of superficial epigastric arteries in early cancer stages. For this, the flow velocity and resistive index of the cranial and caudal superficial epigastric arteries of 63 female canines were evaluated by Doppler ultrasound. The mammary tumor group comprised 43 canines with the histopathological diagnosis of mammary carcinoma, whereas the control group comprised 20 healthy canine. The vascular dynamics was significantly different between the two groups, and the number of tumor lesions affected the vessel flow rate. In addition, the echotexture and presentation and distribution of the vessels affected the resistive index in the mammary carcinoma group. Fifty other female canines were divided into two groups (13 healthy canines and 37 canines with mammary carcinoma) to evaluate the clinical usefulness of the serum measurement of VEGF, interleukin-8, and estradiol, combined with ultrasound examination of malignant tumors. The results demonstrated the strong correlation of echotexture with interleukin-8 levels and the positive correlation between tumor vessel flow rate and VEGF levels. These findings indicate a relationship between the tumor environment and expression of interleukin-8 as well as the effect of flow dynamics on VEGF levels. Finally, 142 mammary nodules or masses were evaluated by ultrasound to assess tumor flow dynamics and differentiate between benign and malignant mammary tumors. The biodynamics of internal vessels was significantly different between benign and malignant tumors, with systolic and diastolic velocities varying according to tumor size and echotexture. Therefore, the joint evaluation of tumor size and texture and of the flow velocity of internal tumor vessels may be useful for differentiating between benign and malignant mammary tumors. The present study presents an important application of ultrasound imaging in veterinary oncology and demonstrates the effect of hemodynamics on cranial and caudal superficial epigastric arteries, evidenced by Doppler ultrasound, in canine mammary carcinoma, particularly when associated with the analysis of tumor size and texture, and of the presentation and distribution of tumor vessels. These findings confirm that mechanical factors of tumors interfere in the hemodynamics of superficial epigastric arteries. These results indicate the importance of evaluating the arteries that irrigate the affected mammary chain together with other factors predictive of tumor malignancy, including tumor size, heterogeneous echotexture of the tumor stroma, heterogeneous presentation and complex distribution of tumor vascularization, and serum levels of VEGF and interleukin-8.

Keywords: Vascularization, Heterogeneous echotexture, Flow velocity, Resistive index.

LISTA DE ABREVIATURAS E SIGLAS

θ	Ângulo de insonação
AEca	Artéria Epigástrica Caudal
AEcr	Artéria Epigástrica Cranial
ANOVA	Análise de Variância
CEUA	Comissão de Ética no Uso de Animais
CM	Neoplasma Mamário
DVI	Distribuição Vascular Interna
DVM	Distribuição Vascular Mista
DVP	Distribuição Vascular Periférica
E2	Estradiol
ELISA	Ensaio de Imunoabsorção Enzimática
GM	Glândula Mamária
GC	Grupo Controle
GNM	Grupo Neoplasma Mamário
HV	Hospital Veterinário
IL-8	Interleucina-8
IR	Índice de Resistividade
M	Metástase
MHz	Megahertz
N	Linfonodo
nm	Nanómetro
PRF	Frequência de Repetição de Pulso
PV	Padrão Vascular
PVTM	Padrão Vascular Tipo Mancha
PVTR	Padrão Vascular Tipo Rede
rpm	Rotações por minuto
T	Tamanho
NM	Neoplasma Mamário
NMb	Neoplasma Mamário Benigno
NMm	Neoplasma Mamário Maligno
NMC	Neoplasma Mamário Canino
NMCb	Neoplasma Mamário Canino Benigno
NMCm	Neoplasma Mamário Canino Maligno
UPF	Universidade de Passo Fundo
VEGF	Fator de Crescimento Endotelial Vascular
Vfl	Velocidade de Fluxo
PVS	Pico de velocidade sistólica
EVD	Velocidade diastólica final
VN	Vascularização Neoplasma

SUMÁRIO

1 APRESENTAÇÃO 8
1.1 INTRODUÇÃO 9
1.2 REFERENCIAL TEÓRICO 10
1.2.1 Tumor mamário canino 10
1.2.2 Vascularização do tumor mamário canino 11
1.2.3 Fatores hemodinâmicos do tumor mamário canino 12
1.2.4 Mensurção sérica do Fator de Crescimento Endotelial Vascular 14
1.2.5 Mensuração sérica da Interleucina-8 15
1.3 PROPOSIÇÃO **..... 15**
1.4 MATERIAIS E MÉTODOS 16
1.4.1 Animais 16
1.4.2 Estudo ultrassonográfico 17
1.4.3 Mensuração sérica do Fator de crescimento endotelial vascular, Interleucina-8 e Estradiol 19
2 ARTIGO 1 - DOPPLER ULTRASOUND ASSESSMENT OF EPIGASTRIC ARTERIES IN CANINE MAMMARY NEOPLASM…….……20
3 ARTIGO 2 - DOPPLER ULTRASOUND AS A TOOL FOR DIFFERENTIATION BETWEEN BENIGN AND MALIGNANT CANINE MAMMARY NEOPLASM.....…45
4 ARTIGO 3 - SERUM MEASUREMENT OF VASCULAR ENDOTHELIAL GROWTH FACTOR, INTERLEUKIN-8 AND ESTRADIOL, AND THE ULTRASOUND FINDINGS OF CANINE MAMMARY NEOPLASM……66
5 DISCUSSÃO 671
6 CONCLUSÃO 94
REFERÊNCIAS 95

1 APRESENTAÇÃO

Esta tese demonstrará na forma de três artigos os resultados obtidos a partir de uma pesquisa sobre a dinâmica de fluxo das artérias epigástricas superficiais cranial e caudal, os atributos vasculares e da textura tumoral ao Doppler ecográfico e a quantificação sérica do fator de crescimento endotelial vascular e da interleucina-8, nos casos de neoplasma mamário canino em estádios oncológicos iniciais.

Os artigos foram estruturados conforme as normas das revistas para as quais foram submetidos. Em vista disso, o primeiro artigo (DOPPLER ECOGRAPHY FOR DIFFERENTIATING BENIGN AND MALIGNANT CANINE MAMMARY TUMORS), está exposto em conformidade com a *Research in Veterinary Science*, ao passo que, o segundo artigo (SERUM MEASUREMENT OF VASCULAR ENDOTHELIAL GROWTH FACTOR, INTERLEUKIN-8 AND ESTRADIOL, AND THE ECOGRAPHIC FINDINGS OF CANINE MAMMARY NEOPLASM) apresenta se em concordância com a *BMC Cancer* e o terceiro artigo (B-MODE AND DOPPLER ECOGRAPHY FOR EVALUATING EPIGASTRIC ARTERIES IN CANINE MAMMARY NEOPLASM), encontra-se de acordo com a *Veterinary and Comparative Oncology*.

O estudo foi desenvolvido no Setor de Diagnóstico por Imagem do Hospital Veterinário da Universidade de Passo Fundo, com auxílio dos Laboratórios de Análises Clínicas, Patologia Animal e Ictiopatologia sob orientação da professora Cinthia Melazzo de Andrade. E para a elaboração da tese, foi utilizado o Manual de Dissertações e Teses da Universidade Federal de Santa Maria 2015.

Por fim, foram apresentados os elementos DISCUSSÃO da tese, que estabelece uma relação entre os artigos desenvolvidos, integrando e argumentando a temática e os resultados finais e REFERÊNCIAS, relacionadas ao conteúdo bibliográfico utilizado para desenvolver os itens INTRODUÇÃO, REFERENCIAL TEÓRICO, MATERIAIS E MÉTODOS e DISCUSSÃO.

1.1 INTRODUÇÃO

O carcinoma mamário (CM) é o neoplasma das mamas, com maior prevalência na espécie canina. O CM tem origem epitelial, evolução clínica variável e diagnóstico confirmado através de exame histopatológico (CLEMENTE et al., 2010; DIESSLER et al., 2017; SANTOS et al., 2013).

O diagnóstico precoce e o tratamento bem-sucedido são prioridades na promoção da sobrevida das pacientes (QUEIROGA et al., 2011). A remoção cirúrgica é o tratamento de eleição. No entanto, o envolvimento dos linfonodos regionais e o desenvolvimento de metástase, limita a cura (CLEMENTE et al., 2010b; DIESSLER et al., 2017; SANTOS et al., 2013). Por isso, as buscas pela identificação do comportamento clínico do CM permanecem sob investigação (PEREZ-RIVAS et al., 2012; SANTOS & MATOS, 2015). Pois, a expansão da compreensão do seu comportamento pode proporcionar uma oportunidade antecipada para intervenções diagnósticas e terapêuticas. Além de tudo, o TMC é um modelo apropriado para o estudo da biologia do câncer e de agentes terapêuticos (QUEIROGA et al., 2011).

Dentre as diversas particularidades dos neoplasmas, a vascularização tem sido um atraente alvo dos estudos sobre diagnóstico e terapia adjuvante (CARMELIET & JAIN, 2011). A vascularização, já foi relatada como preditiva de malignidade, baseada no princípio que o suprimento sanguíneo é crucial para o crescimento, invasão, proliferação e formação do foco metastático (NAGY et al., 2010; CARMELIET & JAIN, 2011; LOGSDON et al., 2014; SANTOS & MATOS, 2015).

A vasculogênese tumoral pode ocorrer por vários mecanismos distintos, que permitem transformar um tumor avascular para um fenótipo vascular, sob a influência de diversos fatores tumorais, principalmente quando há a necessidade do incremento metabólico para as células cancerosas (AUGUSTE et al., 2005; NAGY et al., 2010; LOGSDON et al., 2014; CLEGG & GANHANN, 2015; SANTOS & MATOS, 2015). Entretanto, os tumores podem envolver uma diversidade de vasos, sobretudo revestidos por células tumorais e endoteliais, que por vezes, são precários em desempenhar suas funções (AUGUSTE et al., 2005; NAGY et al., 2010; HOLOPAINEN et al., 2011) e fatores mecânicos teciduais (ZHOU et al., 2014), que constantemente adaptam a vascularização.

Em virtude dessa diversidade e do incremento de vasos serem reconhecidos nos neoplasmas, alguns estudos já foram realizados para caracterizar a vascularização ao exame ultrassonográfico das mamas (HUANG et al., 2013; FELICIANO et al., 2017; THEEK et al., 2017) e, nesse ponto, as técnicas de imagem têm sido indicadas na descrição vascular de forma

não invasiva (YONGFENG et al., 2016; FELICIANO et al., 20017; SOLER et al., 2016; THEEK et al., 2017). Os achados de imagem frequentemente indicam a presença de vascularização, vasos anormais e fluxo intenso, enquanto que, nas neoplasias benignas, observa-se fluxo reduzido, com precária detecção pelo Doppler ultrassonográfico (OK-CHAO et al., 1999; DEL CURA et al., 2005; CANDELARIA et al., 2013; DAVOUDI et al., 2014; YONGFENG et al., 2016). Contudo, não há estudos até o momento sobre o impacto hemodinâmico ao Doppler ultrassonográfico, do CM canino, sobre os principais artérias que dão o aporte sanguíneo para as glândulas mamárias.

Permeando a ausência de dados clínicos sobre essas artérias, que suprem as mamas acometidas por CM, o objetivo deste estudo foi avaliar a hemodinâmica das artérias epigástricas superficiais cranial e caudal ao Doppler ultrassonográfico e identificar atributos vasculares e ecográfico dos CM em estádios oncológicos iniciais, que poderiam contribuir com a interpretação das velocidades de fluxo e do índice de resistividades das artérias estudadas.

1.2 REFERENCIAL TEÓRICO

1.2.1 TUMOR MAMÁRIO CANINO

A glândula mamária (GM) é uma glândula sudorípara modificada, e consiste de parênquima, estroma, ductos, vasos e nervos. As cadelas geralmente têm dois pares de GMs torácicas, dois pares de GMs abdominais e um par de GMs inguinal. Os alvéolos e os ductos são compostos de células epiteliais e revestido por células mioepiteliais. O estroma é relativamente esparso e bem vascularizado. Os septos interlobulares são formados por tecido conjuntivo e fibras elásticas (SORENMO et al., 2011).

Diferentes artérias suprem as GMs. As glândulas torácicas craniais e caudais recebem sangue através das artérias epigástricas superficiais craniais (AEcr), bem como através de ramos das artérias torácicas e intercostais laterais. As glândulas abdominais craniais são suprida pela AEcr e pela artéria epigástrica superficial caudal (AEca). E as glândulas abdominal caudal e inguinal são supridas principalmente pelas AEca e pequenos ramos de outras artérias (Figura). Algumas ramificações acabam cruzado a linha média e irrigando também as GMs contralaterais. O retorno venoso das GMs é paralelo ao suprimento arterial. No entanto, as veias são mais volumosas e têm mais anastomoses em comparação com as artérias. Assim como as artérias, porém com mais frequência, as veias cruzam a linha média (SLEECKX et al., 2011).

Os tumores mamários caninos (TMCs) são as neoplasias mais comuns nas cadelas intactas e as GMs abdominais e inguinais são frequentemente afetadas (SLEECKX et al., 2011). Boa parte dos cães com TMCs têm múltiplas lesões e diferentes tipos e graus histológicos, no momento do diagnóstico (CAVALCANTI & CASSALI, 2006), entretanto a maioria desses tumores, são carcinomas mamários (CMs). As fêmeas acometidas geralmente são mais velhas (QUEIROGA et al., 2011) e comumente apresentam nódulos circunscritos, com tamanho, consistência e mobilidade variável, que podem estar associados a ulceração cutânea e a reação inflamatória (CASSALI et al., 2014).

A cirurgia continua sendo o tratamento de eleição para os TMCs, exceto quando há presença de metástases e no CM inflamatório (CASSALI et al., 2014). A excisão cirúrgica permite o diagnóstico histopatológico e pode ser curativa nos casos de neoplasia benigna e aproximadamente 50% das neoplasias malignas. Os outros 50%, das pacientes estão relacionadas ao desenvolvimento de micrometástase ou recorrência do câncer (CLEMENTE et al., 2010; DIESSLER et al., 2017).

1.2.2 VASCULARIZAÇÃO DOS NEOPLASMAS MAMÁRIOS CANINOS

Dentre as diversas particularidades dos neoplasmas, a vascularização tem sido um atraente alvo dos estudos sobre o diagnóstico e a terapia adjuvante (CARMELIET & JAIN, 2011). No neoplasma a vascularização e a perfusão tecidual podem ser determinantes na detecção e no tratamento, pois é a principal via para os agentes de imagem e drogas anti-tumorais (GOMPPER & FEDOSON, 2015). A vascularização, já foi relatada como preditiva de malignidade, baseado no princípio que o suprimento sanguíneo é crucial para o crescimento, a invasão, a proliferação e a formação de um foco metastático (NAGY et al., 2010; CARMELIET & JAIN, 2011; LOGSDON et al., 2014; SANTOS & MATOS, 2015). Além disso, a neoplasia maligna está relacionada ao maior número de vasos, área e perímetro vascularizado (SLEECKX et al., 2014) e incremento de fluxo sanguíneo (SOLER et al., 2016), em comparação a neoplasia benigna (SLEECKX et al., 2014; SOLER et al., 2016).

A estruturação dos vasos tumorais ocorre a partir de diversos processos, como a angiogênese, o mimetismo vascular, o recrutamento de angioblastos e a cooptação vascular (AUGUSTE et al., 2005). Esses mecanismos permitem transformar um tumor avascular, cujo tamanho seja inferior a 3 mm^3, para um tipo vascular sob a influência da sua demanda metabólica (AUGUSTE et al., 2005; NAGY et al., 2010; LOGSDON et al., 2014; CLEGG &

GANHANN, 2015; SANTOS & MATOS, 2015). Após o estímulo inicial metabólico, a intensidade de neovascularização é variável e dependente das células cancerosas, endoteliais e do microambiente tumoral (HANAHAN & WEINBERG, 2011; CANDELARIA et al., 2013; SAPONARO et al., 2013; SANTOS & MATOS, 2015).

Conforme progride a lesão neoplásica, a vascularização sofre adaptações, para atender a eleva demanda das células e do microambiente em expansão. Entretanto, com vasos diferentes dos homólogos normais em relação a organização, estrutura e função e por isso, nem sempre conseguem suprir as novas e constantes exigências do tecido neoplásico (AUGUSTE et al., 2005; CLEGG & MAC GABHANN, 2015; LOGSDON et al., 2014; NAGY et al., 2010; STEFANINI et al., 2012).

A vascularização pode envolver basicamente três tipos de vasos. Os vasos revestidos por células tumorais, os vasos mosaicos e os vasos dependentes do endotélio. No estroma, os vasos podem apresentar-se aberrantes, numerosos, distorcidos, com porções dilatadas e outras colapsadas, revestimento celular insuficiente, excesso de ramificações, shunts, distribuição espacial complexa e fluxos anômalos (AUGUSTE et al., 2005; NAGY et al., 2010; LOGSDON et al., 2014; SLEECKX et al., 2014; VIGER et al., 2014; CLEGG & MAC GABHANN, 2015). Com isso as neoplasias, frequentemente apresentam má perfusão, insuficiência metabólica, hipóxia, isquemia e necrose (AGUSTE et al., 2005). Além disso, a dinâmica do fluxo gerada nestes vasos, pode possibilitar maior contato entre a circulação e as células cancerosas (RESTUCCI et al., 2002; HOLOPAINEN et al., 2011; VIGER et al., 2014; LI et al., 2016).

As células que compõem os vasos anormais são capazes de interagir e se adaptar com as adversidades do microambiente do câncer (AUGUSTE et al., 2005; CLEGG & MAC GABHANN, 2015; LOGSDON et al., 2014; NAGY et al., 2010; SLEECKX et al., 2014; VIGER et al., 2014). A resposta imunológica, a hipóxia, a demanda metabólica e a biomecânica das neoplasias são atribuições associadas a manutenção e ao incremento do aporte e fluxo sanguíneo, por interferirem na expressão de fatores pró-angiogênico, particularmente pelas células cancerosas (NAGY et al., 2010).

1.2.3 FATORES HEMODINÂMICOS DO NEOPLASMA MAMÁRIO CANINO

Os neoplasmas malignos geralmente são vascularizados, possuem sinais de fluxo enriquecido e são constituídos de vasos anormais e pouco efetivos (OK-CHAO et al., 1999; DEL CURA et al., 2005; CANDELARIA et al., 2013; DAVOUDI et al., 2014; YONGFENG

et al., 2016). Desta forma, apresentam com maior frequência alterações na dinâmica de fluxo, particularmente quando relacionado ao estresse tecidual (NAGY et al., 2010; CLEGG & GABHANN., 2015). Os principais fatores biomecânicos que interferem na hemodinâmica incluem o esforço de cisalhamento e a tensão circunferencial do fluxo nas vias vasculares, a concentração de células sanguíneas, a viscoelasticidade do tecido adjacente e a constituição da parede dos vasos (CARMELIET, 2000; LEE et al., 2010; CLEGG & GABHANN., 2015; GOMPPER & FEDOSON, 2015). Esses estímulos são constantes e colaboram com a formação, remodelamento e manutenção dos vasos tumorais (CLEGG & GABHANN., 2015).

A ultrassonografia é um método indicado, na detecção e caracterização da vascularização do neoplasma (CANDELARIA et al., 2013; GOKALP et al., 2009; LEE et al., 1996; LOH et al., 2009). Os neoplasmas malignos geralmente apresentam vascularização, aumento do número de vasos, vasos tortuosos, distribuição vascular complexa, excesso de ramificações (Figura), entre outros atributos, que contrapõem os achados no TMCb, que além disso em maior proporção está associado ao baixo fluxo detectável ao Doppler (OK-CHAO et al., 1999; DEL CURA et al., 2005; CANDELARIA et al., 2013; DAVOUDI et al., 2014; YONGFENG et al., 2016).

Outro fator que pode ser associado a hemodinâmica do fluxo dos vasos do neoplasma é a pressão sólida gerada pelas células cancerosas, estroma e interstício, que comprimem externamente os vasos. Os neoplasmas benignos são considerados menos rígidos, pois apresentam menor proliferação celular e as reações estromais, associadas a insuficiência metabólica, hipóxia, isquemia e necrose são inconstantes e menos frequentes. Nos neoplasmas malignos, há maior proliferação das células cancerosas e as reações de amparo tecidual são mais intensas. Essas reações no neoplasma maligno contribuem para a formação de sua heterogeneidade (Figura), rigidez e pressão interna. Através, do aumento da densidade celular, aumento de colágeno depositado, formação de focos de fibrose, maior proporção de fluídos, proteínas plasmáticas e células sanguíneas no interstício tumoral, além de maior comprometimento dos tecidos adjacentes na região de malignidade (ZHOU et al., 2013; FELICIANO et al., 2014).

Essas anomalias vasculares e teciduais produzem alterações na dinâmica do fluxo, a partir do incremento das forças mecânicas, particularmente o cisalhamento e a tensão circunferencial (CLEGG & GABHANN., 2015). Além disso, as variações de fluxo ativam as células da parede vascular que se adaptam estruturalmente e funcionalmente através de estímulos pró angiogenese (HOLOPAINEN et al., 2011; VIGER et al., 2014; MORI et al., 2017).

1.2.4 MENSURAÇÃO SÉRICA DO FATOR DE CRESCIMENTO ENDOTELIAL VASCULAR

A angiogênese é o mecanismo primordial da vascularização do neoplasma e envolve a formação e a organização de novas estruturas vasculares, a partir de vasos sanguíneos pré-existentes (FOLKMAN, 1996; RESTUCCI et al., 2000; HOLOPAINEN et al., 2011). O fator de crescimento endotelial vascular (VEGF) é o principal estimulante desse mecanismo de vascularização. O VEGF é uma citocina pró-angiogênica potente, que está envolvida no aumento da permeabilidade, na migração e proliferação de células endoteliais, na maturação das novas vias vasculares, na produção de moléculas vasoativas e na estimulação da quimiotaxia monocitária (AUGUSTE et al., 2005; KATO et al., 2007; MILLANTA et al., 2010; SANTOS et al., 2010; SAPONARO et al., 2013).

O VEGF pode ser produzido por células cancerosas, endoteliais e do microambiente tumoral e sua secreção é desencadeada por uma série de estímulos moleculares, incluindo outras citocinas e fatores de crescimento, hipóxia, hormônios, perda de função p53 e mutações (ANGELO & KURZROCK, 2007; FAN et al., 2012). As células cancerosas produzem VEGF, mas não respondem diretamente, porque não possuem receptores na sua superfície. Em contraste, as células endoteliais expressam receptores, mas produzem muito pouco VEGF (KERBEL, 2008). A maior expressão de VEGF foi relatada nos neoplasmas sólidos, quando relacionado a vascularização composta por vasos anormais e pouco funcionais. Com isso, a concentração sérica do VEGF elevada foi relacionada como um parâmetro clínico patológico de pior prognóstico e menor taxa de sobrevivência nas neoplasias mamárias (DURANYILDIZ et al., 2008; SHIVAKUMAR et al., 2008; MOHAMED ALI et al., 2011).

Outro fator envolvido, na expressão do VEGF, porém pouco citado, é a pressão sólida gerada no ambiente tumoral. Esse estímulo mecânico produzido está associado a maior compressão do meio extra vascular sobre os vaso e prejuízo no fluxo de fluído interno. Esse estresse biodinâmico pode se tornar crônico, com a evolução do neoplasma, devido a proliferação e o amparo tecidual resultante das constantes reações estromais. Com isso, desenvolve-se baixa perfusão tecidual, pelo aumento da pressão do estroma e do interstício. O resultado desses eventos, podem estar relacionados ao incremento do VEGF, com o intuito de "normalizar" a circulação e a perfusão e contornar o déficit metabólico e a hipóxia tecidual (JAIN, 2005; SANTOS et al., 2010; SILVESTRE et al., 2013).

Os hormônios esteroides sexuais, também devem ser investigados em conjunto com o

VEGF, pois são fundamentais na mamogogênese, principalmente no desenvolvimento do tecido lóbulo-alveolar (QUEIROGA et al., 2011). Em humanos, foi proposta a influência dos esteroides sexuais na expressão do VEGF, devido ao aumento vascular da mama perante a estimulação esteroide (HYDER, 2006; SANTOS et al., 2010), podendo desta maneira, sobrepor ainda mais a expressão do VEGF no TM, particularmente quando desencadeada pela interação do complexo ERα/estradiol (FAN et al., 2012).

1.2.5 MENSURAÇÃO SÉRICA DA INTERLEUCINA-8

O sistema imunológico reage à presença do neoplasma e indiretamente acaba favorecendo o incremento de fatores pró oncogênese, como a interleucina-8 (DIRKX et al., 2006; DERIN et al., 2007). A interleucina-8 (IL-8) é uma citocina pró inflamatória e pró angiogênica, relacionada ao crescimento, sobrevivência, invasão, angiogênese, metástase, resistência e recorrência neoplásica (LEE et al., 2012; MOHAMED et al., 2013). A expressão elevada de IL-8 e seus receptores tem sido identificada em células cancerosas, endoteliais, mastócitos, neutrófilos e macrófagos, particularmente em condições associadas a processos inflamatórios e de hipóxia tumoral (SHAHZAD et al., 2010; MOHAMED et al., 2013; DIRKX et al., 2014). Por esses motivos, a IL-8 é considerada um fator regulador das variações do microambiente tumoral (YUAN et al., 2005; LEE et al., 2012; RAPOSO et al., 2015).

O incremento sérico da IL-8, já foi relatado quanto a presença de neoplasmas malignos (LIN et al., 2004; WAUGH & WILSON, 2008; ZUCCARI et al., 2011), associados a inflamação (SHAHZAD et al., 2010; MOHAMED et al., 2013; DIRKX et al., 2014), a hipóxia (ANGELO & KURZROCK, 2007; GILKES & SEMENZA et al., 2013; SILVESTRE et al., 2013), metástase local e distante (GELALETI et al., 2012; ANDRÉS et al., 2013; MA et al., 2017). Entretanto, os dados sobre a quantificação da IL-8 no soro das cadelas com neoplasma mamário malignos é escassa. Os poucos estudos mostraram níveis séricos maiores nas neoplasias malignas, quando comparado com pacientes saudáveis (GELALETI et al., 2012; ANDRÉS et al., 2013). Os mesmos achados sobre a IL-8 em neoplasmas malignos foram encontrados em humanos, entretanto com maior incremento sérico, associados a presença de mestástase local e/ou distante (DERIN et al., 2007; MA et al., 2017; BENOY et al., 2004).

1.3 PROPOSIÇÃO

O objetivo geral desse trabalho foi verificar a hemodinâmica das artérias epigástricas superficiais cranial e caudal a ecografia modo-B e Doppler em cadelas com carcinoma mamário, em estádios oncológicos iniciais e sugerir como método de avaliação de neoplasmas mamários. Quanto aos objetivos específicos da pesquisa científica, procurou se identificar os atributos ecográficos vasculares e da textura dos neoplasmas malignos e a mensuração sérica do fator de crescimento endotelial vascular e da interleucina-8, também nos estádios oncológicos iniciais, que poderiam contribuir com a interpretação das velocidades de fluxo e índice de resistividades das artérias epigástricas superficiais cranial e caudal.

1.4 MATERIAIS E MÉTODOS

A descrição que segue envolve a metodologia empregada nos pacientes referentes aos Artigos 1, 2 e 3.

1.4.1 ANIMAIS

Os animais foram selecionados na cidade de Passo Fundo e região, as quais os tutores tiveram interesse em realizar o exame ecográfico e a mastectomia. O experimento foi aprovado em seus aspectos éticos e metodológicos pela Comissão de Ética no Uso de Animais da Universidade de Passo Fundo (CEUA-UPF), sob parecer número 030/2017. Foram avaliadas 102 cadelas não castradas. O grupo controle (GC) foi constituído por 20 cadelas hígidas submetidas a avaliação pré cirúrgica para a realização da ovário-histerectomia eletiva. Os critérios de exclusão para o GC incluíram sinais de estro, histórico de neoplasia e doença inflamatória recente. Quanto aos animais com tumor mamário, foram incluídos na triagem, após consulta clínica, 82 fêmeas sem histórico de doença inflamatória e estro recente, com nódulo mamário maior que um centímetro no seu maior diâmetro, sem ulceração cutânea, sem sinais inflamatórios e sem indícios de metástase local e distante, nos exames imagem (radiográfia de tórax e ecografia abdominal e linfonodos axilar e inguinal). As avaliações foram realizadas em 2017, no Hospital Veterinário da Universidade de Passo Fundo (HV-UPF).

As fêmeas acometidas por TMs foram submetidas ao procedimento cirúrgico após estadiamento oncológico baseado na versão adaptadada (RUTTEMAN et al., 2001), para neoplasias mamárias. Assim, o tamanho (T) do tumor foi categorizado em T1 (<3 cm), T2 (entre 3 e 5 cm) e T3 (> 5 cm); o envolvimento do linfonodo (N) regional como N0 (ausente) e N1

(presente); e quando metástase (M) distante em M0 (ausente) e M1 (presente). A partir desses, foram caracterizados os estádios 1 (T1, N0 e M0), 2 (T2, N0 e M0), 3 (T3, N0 e M0), 4 (qualquer T, N1 e M0) e 5 (qualquer T, qualquer N e M1). A cadeia de glândulas mamárias e o linfonodo axilar e inguinal foram removidos cirurgicamente e submetidos ao exame histopatológico. Os tecidos após exérese foram fixados em formaldeído 10% e posteriormente embebidos em parafina. Secções histológicas (5 μm de espessura) foram obtidas e coradas com hematoxilina e eosina. A classificação da neoplasia foi realizada de acordo com GOLDSCHMIDT et al. (2011), pelo Laboratório de Patologia Animal do HV-UPF. Com base no diagnóstico histopatológico, o grupo neoplasma mamário (GNM) foi constituído por 43 fêmeas, com diagnóstico anatomopatológico de carcinoma mamário (CM), para o estudo das artérias epigástricas superficiais, 142 neoplasmas mamários para o estudo das características ecográficas vasculares e da textura e 37 cadelas para a mensuração sérica do VEGF, IL-8 e estradiol. A categorização dentro do GNM para o grau histológico e estádio oncológico foi definida pela maior agressividade e maior estádio, quando mais de um neoplasma identificado na cadeia mamária.

1.4.2 ESTUDO ULTRASSONOGRÁFICO

Após a avaliação clínica e antes do procedimento cirúrgico, os TM, bem como os linfonodos regionais, foram examinados com um transdutor linear de 4-13 MHz (Mylab 70, Esaote, Genova, Itália). Os cães foram examinados em decúbito dorsal e não foi necessária a contenção química. Para diminuir a subjetividade do estudo, e como a ultrassonografia é dependente do operador, todos os exames foram realizados pelo mesmo médico veterinário.

Na avaliação dos neoplasmas, foi verificada a ecotextura (homogênea ou heterogênea) em modo-B, a presença ou a ausência de fluxo, a distribuição e a apresentação dos vasos através do Doppler colorido (Figura 2). Na distribuição dos vasos, foi observado a presença de fluxo na periferia e no interior do tumor, sendo categorizado em periférico (DVP), quando vasos somente na periferia da lesão, interno (DVI), na ocorrência exclusiva de vasos no interior, e misto (DVM), nas situações que foram evidenciados vasos periféricos e internos conjuntamente (Figura 2). Apoiado também na identificação do fluxo, foi possível verificar a apresentação dos vasos e propor dois padrões de apresentação vascular (PV) no neoplasma mamário, adaptados do protocolo publicado por Tanaka (1990). O padrão vascular tipo rede (PVTR), para formações tubulares contínuas, numerosas, distorcidas, com diâmetros variados, excessos de

ramificações e distribuição espacial complexa, e o padrão vascular tipo mancha (PVTM), para formações tubulares, ramificadas, com variações de diâmetro e distribuição espacial dispersas (Figura 2).

Na avaliação do linfonodo axilar e inguinal, foram utilizados como critérios de exclusão o formato arredondado, o hilo estreito ou ausente, a hipoecogenicidade do parênquima, as margens afiladas, a presença de reforço acústico posterior e fluxo sanguíneo de distribuição complexa ou periférica (Figura 3), estando essas imagens relacionadas ao acometimento linfático (CARVALHO, 2009).

O exame dos vasos tumorais iniciou em modo-B, obtendo-se imagens em plano longitudinal e transversal, observando-se a parede, o conteúdo luminal, o diâmetro e à reação do vaso a pressão mecânica do transdutor, quando possível. Após, com o Doppler colorido, foi avaliado a presença, direção e características do fluxo e, desse modo, confirmada a passagem luminal. A análise da dinâmica de fluxo vascular foi realizada por Doppler espectral, mantendo o ângulo de insonação (θ) menor de 60 ° e o volume de amostra ajustado ao diâmetro do vaso. O ganho e a frequência de repetição de pulso (PRF) foram refinados de acordo com a velocidade do fluxo (Vfl), sendo avaliado a velocidade sistólica (Vs), a velocidade diastólica final (Vd) e o índice de resistividade (IR = Vs - Vd) / Vs) (CARVALHO, 2009). A análise da dinâmica do fluxo foi verificada somente quando observada a formação de três ondas similares (Figura). Todas as mensurações das Vfl foram repetidas três vezes, empregando a mediana de cada valor para este estudo. As imagens foram armazenadas digitalmente para análises.

O exame das AECr e AECa teve início em modo-B, obtendo-se imagens em plano longitudinal e transversal, observando-se os aspectos ecográficos referentes a parede, ao conteúdo luminal, ao diâmetro e à reação do vaso a pressão mecânica do transdutor. Após, o Doppler colorido foi utilizado para avaliar a presença, direção e características do fluxo arterial e, desse modo, confirmar o fluxo luminal livre. A análise espectral foi realizada mantendo o ângulo de insonação (θ) menor de 60 ° e o volume de amostra ajustado de acordo com o diâmetro do vaso. O ganho e a frequência de repetição de pulso (PRF) foram ajustados de acordo com a velocidade do fluxo, sendo averiguadas quanto a morfologia das ondas, perfil de velocidade de fluxo laminar, Vs, Vd e IR (Figura). A análise da dinâmica do fluxo foi verificada somente quando observada a formação de três ondas similares (Figura). Todas as mensurações das Vfl foram repetidas três vezes. As imagens foram gravadas e armazenadas digitalmente para análises e cálculos subsequentes.

1.4.3 MENSURAÇÃO SÉRICA DO FATOR DE CRESCIMENTO ENDOTELIAL VASCULAR, INTERLEUCINA-8 E ESTRADIOL

Foram coletados três mililitros de sangue em um tubo sem anticoagulante. As amostras foram mantidas em temperatura ambiente por até uma hora, para a retração do coágulo, e centrifugadas a 2.500 rpm, por 5 minutos, para promover a separação do soro. Após pipetagem, o soro foi transferido para um tubo plástico tipo ependorf, identificado e congelado a –20ºC. A mensuração sérica do fator de crescimento endotelial vascular (VEGF) foi realizado empregando o kit Canine VEGF, Quantikine® ELISA (R & D Systems®, Minneapolis, USA), com anticorpo monoclonal específico para VEGF. A mensuração sérica da Interleucina-8 (IL-8) foi realizada empregando o kit Canine CXCL8/IL-8, Quantikine® ELISA (R & D Systems®, Minneapolis, USA), com anticorpo monoclonal específico para IL-8 canina. O nível sérico de Estradiol (E2) foi mensurado através de kit Estradiol, Parameter™ (R & D Systems®, Minneapolis, USA), empregando anticorpo monoclonal específico para Estradiol. As técnicas seguiram as orientações do fabricante, para cada um dos kits. As densidades ópticas foram medidas a 450 nm em um leitor de ELISA (Asys UVM 340). As intensidades das reações foram proporcionais às concentrações de VEGF, IL-8 e Estradiol. O cálculo das densidades ópticas foi determinado através das curvas de ajuste usando o software Plate Digiread®.

2 ARTIGO 1 - DOPPLER ULTRASOUND ASSESSMENT OF EPIGASTRIC ARTERIES IN CANINE MAMMARY NEOPLASM

Artigo submetido no periódico:

Veterinary and Comparative Oncology

Doppler ultrasound assessement of epigastric arteries in canine mammary neoplasm

Abstract

This study aimed to evaluate epigastric arteries in canine mammary carcinoma (MC) using B-mode, color Doppler, and spectral Doppler ultrasound and identify vascular activity. A total of 43 examinations were performed to characterize the echotexture, blood flow, and pattern of vascular presentation in the stroma of the neoplasm. The flow velocities and resistive index of the cranial and caudal epigastric arteries of 63 female dogs were also evaluated. The MC group comprised females with MC whose breasts were removed and submitted to histopathological examination, whereas the control group comprised 20 healthy females. The epigastric vascular dynamics were significantly different between the groups ($p < 0.01$). Flow velocities were influenced by the number of neoplasm, and the resistive index was significantly different in the presence of heterogeneous echotexture and network-type vascular pattern ($p < 0.01$), confirming increased neoplasm flow, vascular changes, increased stiffness, and less viscoelasticity in MC; these characteristics interfered with epigastric artery hemodynamics. Thus, the number of neoplasm, echotexture, and type of vascular pattern associated with epigastric artery hemodynamics can aid in the evaluation of vasculogenesis and are therefore promising indicators of the biological behavior of the neoplasm.

Keywords: female, dogs, mammary carcinoma, hemodynamics, ultrasonography, neoplasms

INTRODUCTION

Mammary tumors (MTs) are common neoplasms in female dogs and approximately half are malignant[1,2]. Mammary carcinoma (MC) is the most prevalent malignant condition. MC has an epithelial origin and variable clinical evolution, and its diagnosis is confirmed by histopathological examination. Although surgical removal is the treatment of choice, the development of local and distant metastasis limit its cure[3-5]. Therefore, the search for identification markers for MC behavior remains under investigation[6,7]. Moreover, canine mammary neoplasia is an appropriate model for the study of cancer biology and cancer therapeutic agents[1].

Benign and malignant neoplasm have different grades of vascular growth. Malignant lesions are usually vascularized, with vessels morphologically and functionally distinct from the normal analogs as well as enriched flow signals[8-10]. This differentiated vascularization in the lesion constantly influences the stroma and vasculogenic activity of the neoplasm[11-14].

Vessel formation is regulated by various stimuli and morphogenic processes[11,13,15,16]. Vascular remodeling by flow hemodynamics, which allows the vascular phenotype to be transformed according to the metabolic demand and the mechanical stress of the vessels, is one such process[12,13,17-20]. Thus, vascular supply in canine MCs is an important target for understanding the biological behavior of the neoplasm as well as indicating future adjuvant therapeutic protocols.

Ultrasonography is a method indicated for the detection of neoplasm vascularization and its morphological characteristics[21-24]. In human medicine, it is indicated as an auxiliary diagnostic technique; however, it is not widely used for evaluating the mammary gland of female dogs[25-27]. Studies have utilized imaging methods to demonstrate the characteristics of vascular flow in mammary neoplasms[26,28-30], which show findings of the internal and peripheral

vessels[26,31], morphological characteristics of the network[9], and neoplasm flow dynamics[26,28] as indicators of malignancy. However, dynamic adaptation of the arteries, which branch out to supply the mammary glands, has not been described. Thus, changes in epigastric artery hemodynamics may reflect the vascular behavior and remodeling in canine MC. Thus, the objective of the present study was to assess the relationship between the hemodynamic findings of the epigastric arteries and oncologic stage, number of neoplasms in the affected mammary chain, histological grade, echotexture, and vascular presentation pattern in canine MC.

MATERIAL AND METHODS

Characterization of the sample

The mammary glands, the cranial epigastric artery (CrEA), and the caudal epigastric artery (CaEA) of 63 intact female dogs were evaluated in 2017 at the Veterinary Hospital of the University of Passo Fundo (VH-UPF). Among the sample, 20 female dogs were healthy and 43 had mannary carcinoma (MC). The control group (CG) comprised 20 healthy female dogs submitted to preoperative evaluation for elective ovary-hysterectomy. Exclusion criteria for the CG included signs of estrus, history of neoplasm, and recent inflammatory disease. The animals with MCs were clinically evaluated, and only females without a history of recent disease and estrus; with a breast neoplasm larger than 1 cm in diameter; and without skin ulcerations, signs of inflammation and local and distant metastasis were not included. The females with MCs were submitted to the surgical procedure after oncologic staging based on the adapted version[32] for epithelial neoplasms. Thus, neoplasm size (T) was categorized into T1 (<3 cm), T2 (3–5 cm) and T3 (>5 cm); the involvement of lymph nodes (N) was classified as N0 (absent) and N1 (local metastasis); and presence of distant metastasis (M) was categorized as M0 (absent) and M1 (present). The former categories were used to characterize

stages 1 (T1, N0, and M0), 2 (T2, N0, and M0), 3 (T3, N0, and M0), 4 (any T, N1, and M0), and 5 (any T, any N, and M1). The mammary gland chain and the axillary and inguinal lymph nodes were surgically removed and submitted to histopathological examination. After excision, the tissues were fixed in 10% formaldehyde and subsequently embedded in paraffin. Histological sections (5-µm thick) were obtained and stained with hematoxylin and eosin. Neoplasms were classified according to Goldschmidt et al.[33] by the Laboratory of Animal Pathology of the HV-UPF. Based on the histopathological diagnosis, the mammary carcinoma group (MCG) comprised 43 females with diagnosis of MC. Stratification within the MCG was defined by the greater aggressiveness and greater stage when there was more than one neoplasm in the mammary chain.

Ultrasonographic study

After the clinical evaluation and before the surgical procedure, the mammary glands, MCs, lymph nodes, and CrEAs and CaEAs were examined with a 4–13 MHz linear transducer (Mylab 70, Esaote, Genova, Italy). The dogs were examined in dorsal recumbence position, and no chemical restraint was required. To reduce the subjectivity of the study all examinations were performed by the same sonographer. For evaluating the glands and breast neoplasms, echotexture and vascularization were assessed by B-mode and color Doppler ultrasound, respectively. The identification of the flow allowed the determination of the formation and distribution of the vessels. Based on these characteristics of the vessels, two patterns of vascular presentation in the MC stroma were proposed: 1) the network-type vascular pattern (NTVP), for several continuous and distorted tubular formations with varying diameters, excess branching, and complex spatial distribution and 2) spot-type vascular pattern (STVP), for branched tubular formations with varying diameter and scattered distribution. For evaluating

the axillary and inguinal lymph nodes, features such as rounded shape, hypoechogenicity of the parenchyma, presence of posterior acoustic enhancement, and peripheral or complex blood flow distribution were used as exclusion criteria[34]. Ultrasound examination of the CrEA and CaEA was initiated in B-mode, and images in the longitudinal and transverse planes were obtained. Afterwards, color Doppler was used to evaluate the presence, direction, and characteristics of the arterial flow and confirm luminal patency. Spectral analysis was performed using an insonation angle (θ) of less than 60°, and the sample volume was adjusted to the vessel diameter. Gain and pulse repetition frequency were adjusted according to the flow velocity, and the investigated parameters were peak systolic velocity (PSV), end diastolic velocity (EDV), and resistive index [RI = (PSV − EDV)/PSV][35]. The aforementioned analyses were performed in thrice, and the results were expressed as mean ± standard deviation. The images were recorded and stored digitally for subsequent analysis and calculations.

Statistical analysis

The variables were tested for their normal distribution using the Kolmogorov–Smirnov test. As a result, the variables PSV and EDV, obtained from both CrEA and CaEA, followed a Gaussian distribution. Analysis of variance (ANOVA) was performed, followed by Tukey's post-hoc test to compare the groups. However, the RI variables, both in the CrEA and CaEA, did not follow a normal distribution, and the Kruskal–Wallis test was used, followed by Dunn's multiple comparison post-hoc test. P values <0.05 were considered statistically significant. The GraphPad Prism® software, version 6.0, was used for statistical analysis.

The study protocol was in accordance with the ethical principles for the use of laboratory animals of the Brazilian Society of Science in Laboratory Animals and was approved by the Ethics Committee on Animal Use (UPF), Passo Fundo, RS, Brazil.

RESULTS

Characterization of glands

A total of 63 female dogs aged 3–15 years (mean age of 10.6 years in the CG and 10 years in the MCG) were evaluated. In the CG, no clinical and ultrasonographic changes were identified in the tissue and blood vessels of the mammary glands. In the MCG, the prevalence of one lesion was the highest. With regard to the regional distribution of MCs, abdominal mammary glands were the most affected, followed by thoracic and abdominal, abdominal and inguinal, and only one thoracic mammary gland. According to the oncological evaluation, there was a predominance of stage II carcinoma, followed by stage I and stage III carcinomas. Based on the histopathological diagnosis, the MCG was predominantly composed of grade I carcinomas, followed by grade II, ungraded, and grade III carcinomas.

On ultrasonographic examination of MCs, heterogeneous echotexture predominated over homogeneous echotexture. It was not possible to identify vascular flow in one case of grade I carcinoma (stage I) in the thoracic region. The identification of the distribution of internal and peripheral (mixed) vascularization was absolute for cases in which vascular flow could be identified. Neoplasm stromal vessels were most frequently presented in an NTVP and the remainder in a STVP. The echogenicity and echotexture of the ultrasonographic images of inactive mammary tissue were similar to those of adjacent fat and vessels with morphology, distribution, and flow preserved on Doppler.

Ultrasonography of the epigastric arteries

In the ultrasound evaluation of the CrEAs and CaEAs of the 63 canine females included in this study, there were no abnormalities in the wall, luminal content, direction of flow, and reaction to the mechanical pressure of the transducer. Hemodynamic evaluation showed a significant difference in the flow velocities (flV), with higher peak systolic velocity (PSV) in the CrEA ($p < 0.01$) and CaEA ($p < 0.01$) in the MCG than in the CG. Conversely, a significant difference in diastolic velocity (EDV) was only observed for the CaEA ($p < 0.01$) in the MCG in comparison to the CG. The EDV of CrEA was not significantly different ($p > 0.05$) between the CG and MCG (Figure 1). The vascular RI was increased both in the CrEA ($p < 0.01$) and CaEA ($p < 0.01$) of female dogs diagnosed with MC in comparison to healthy females (Figure 2). After stratification according to the number of neoplasms, oncological stage, stroma echotexture, vascular pattern, and histopathological grade, significant differences were observed in flV and IR of the CrEA (Table 1) and CaEA (Table 2) between the groups.

In the CrEA, PSV and RI were higher in cases diagnosed with MC with one and two neoplasms than in the CG ($p < 0.01$); however, there was no difference between cases with the highest number of lesions and the CG ($p > 0.05$). Nevertheless, no difference was observed in EDV between the CG and the number of MCs in the mammary chains of dogs in the MCG. An increase in flV and RI was observed in the CaEA. The PSV was significantly different between the CG and MCG with respect to the number of MCs, with ≥3 neoplasmas having the highest PSV, followed by 2 neoplasms, 1 neoplasm, and CG ($p < 0.01$). Similarly, the EDV was significantly different between the CG and MCG with respect to the number of MCs ($p < 0.01$), with ≥3 neoplasms and 2 neoplasms having the highest EDV, followed by 1 neoplasm and CG. However, there was no significant difference in EDV between 2 neoplasms and ≥3 neoplasms ($p > 0.05$). The RI was only different between the CG and the MCG regardless of the number of neoplasms ($p < 0.01$).

In CrEA the PSV result was higher in stage III than that in the CG and stages I and II ($p < 0.01$). Moreover, EDV did not increase in the CrEA, and there were no differences between the stages. There were no differences between the CG and the stages ($p > 0.05$). Despite this, the RI in CrEA was higher in stages I, II, and III in comparison to the CG ($p < 0.01$) but with no statistical difference between stages ($p > 0.05$). In the CaEA, PSV, EDV, and RI were higher than those in the CG ($p < 0.01$), regardless of the stage, but were not different from each other ($p > 0.05$).

In the presentation of the echotexture of the neoplasm stroma, interferences with the flV and RI in the epigastric arteries were also evidenced. In the CrEA, PSV was higher in heterogeneous MC than in the CG ($p < 0.01$) and there were no differences between heterogeneous and homogeneous MC as well as homogeneous MC and the CG ($p > 0.05$). Regardin to EDV results, no difference was observed between the echotextures and the CG ($p > 0.05$). However, the RI of the heterogeneous and homogeneous MCs exceeded that of the CG ($p < 0.01$) and were not different from each other. In the CaEA, the RI was higher in the heterogeneous MC, followed by the homogeneous MC, and lower in the CG ($p < 0.01$). The PSV and EDV did not differ between the echotextures, but they were higher than those in the CG ($p < 0.01$).

The PSV and RI in the CrEA was lower in the CG in comparison to the patterns of vessel presentation inside the MC ($p < 0.01$), and no differences were observed within the MCG ($p > 0.05$), even with EDV showing no significant difference between CG and the NTVP and STVP ($p > 0.05$). The NTVP was predominant in the MCG, and the RI in the CaEA was higher in the NTVP than in the STVP and the CG ($p < 0.01$). The RI in the STVP was increased relative to that of the CG ($p < 0.01$) because the PSV and EDV of the patterns were higher than those of the CG ($p < 0.01$), although not different from each other ($p > 0.05$).

Furthermore, flow dynamics differed according to the histological grade because the PSV in the CrEA was higher in MC grades I and II and ungraded MC than in the CG ($p < 0.01$). In contrast, no difference was observed between the CG and ungraded MCs ($p > 0.05$). However, EDV did not differ between the histological grades and the CG ($p > 0.05$). Nevertheless, the RI in MC grade I, grade II, and ungraded MC increased, in contrast to the CG ($p < 0.01$). In the CaEA, the PSV, EDV, and RI of MC grade I and II and ungraded MC were higher than those of the CG ($p < 0.01$) but with no differences between the grades ($p > 0.05$).

DISCUSSION

MC is the malignant mammary neoplasm with the highest incidence in female dogs[4]. In our study, the MCG included only females with a diagnosis of MC. Moreover, the groups included adult females of different breeds because there is no predilection [2], and breast neoplasms in intact female dogs are predominant in adult and older individuals[1,2,4,36]. The MCG included 43 dogs with MC of different grades and ungraded that underwent histopathological examination, which is the gold standard in the diagnosis of epithelial neoplasms[33,36]. The most commonly affected breasts are the abdominal and inguinal glands[2], in which solitary neoplasm and clinical stage II are predominantly detected. This fact may be associated with the significant hemodynamic findings in the CaEA because it is the main supply vessel of the abdominal and inguinal mammary glands[2].

The main biophysical factors that may interfere with the vascular hemodynamics of a tissue include shear stress and circumferential tension of blood vessels[37-39]. In our study, an evaluation and interpretation of the sonographic characteristics of the vasculature architecture in the CrEA and CaEA was performed to investigate the characteristics of the MC. The hemodynamic changes on the spectral Doppler were related to the increase in shear stress and

circumferential tension resulting from greater flow demand, excess branching, loss of viscoelasticity associated with greater stiffness, and interstitial pressure generated by reactions in the stroma of the MC.

The initial characteristic evaluated was the presence of blood flow in the mammary gland as well as inside the MC and the adjacent area. Malignant MNs are vascularized due to the greater blood supply that is required for stromal proliferation, growth, and viability[16,20,40]; this was confirmed in relation to the MC in almost all cases. Additionally, the identification of internal and peripheral vessels confirmed increased flow in MCs. This has been reported in other studies with malignant solid neoplasms, which have related aggressiveness to the detection of increased flow. It has been proposed that the main reason for this association is tissue perfusion demand, metabolic requirement[8-10,21,25,26,41,42], and chronic mechanical stress[11,12,28,43] during cancer progression. This inclusion of flow results in an increase in shear stress and circumferential tension in the arteries that irrigate the tissue[11,13,44,45], thereby leading to changes in flow dynamics. It was therefore possible to verify this peculiarity of MCs and observe increased hemodynamic values (flV and IR) in the epigastric arteries. The number of neoplasms in the MCG was associated with the adaptations of the flV and IR because the CrEA received a smaller stimulus probably due to the decreased involvement of the mammary glands, which contradicts the findings in the CaEA associated with a greater number of MCs in the abdominal and inguinal mammary glands. In the CaEA, the flV followed the demand for irrigation to the higher number of lesions; the flow velocities were lower in the absence of lesions and were higher in the presence of two or three neoplasms. However, the increase in flow due to the higher number of MCs did not reflect on the RI.

In addition to malignancy, size may be related to increased vascular flow and volume[11,13,14,44,45], with the epigastric arteries adapting to the shear stress and circumferential tension. Therefore, flV and RI were compared between the CG and the stages as well as between

stages I, II, and III, and it was possible to perceive the influence of the presence and size of the lesion on vascular flow dynamics. In all three stages, the RI was higher in the CrEA and CaEA than in the healthy mammary tissue and the flVs were increased in the CaEA. However, when accounting for the size of the lesions, the PSV was different in the CrEA only in stage III, which may be associated with a greater flow demand to larger masses[41].

In addition to blood flow and neoplasm size, other factors may affect the shear stress and the circumferential tension of the epigastric arteries. Stromal pressure on the vessels is one of these factors[11]. The dynamics of the vessels that irrigate the MC were affected by the echotexture of the stroma. The difference in PSV and RI between heterogeneous and homogeneous carcinomas and the CG may be attributed to the higher mechanical pressure of the MC on the vessel wall, with stiffness and viscoelasticity being conditions associated with malignancy[28]. Thus, the evaluation of MC echotexture complements our understanding of the hemodynamic variations in the epigastric arteries because flow dynamics can adapt and shape the flV of the formed mammary branches. Neoplastic vessels are reported to be poorly effective and are therefore frequently associated with lesions due to metabolic insufficiency, hypoxia, ischemia, and necrosis[11,19,46-49], which generate additional reactions in the stroma of the neoplasm that modify the echotexture. These characteristics are related to increased collagen deposition, formation of fibrotic foci, cell density and proportion of fluids, plasma proteins, and blood cells in the neoplasm environment[43]. Imaging techniques have already been used to detect the morphological and functional aspects of the vessels MNs[8, 10,21,26,28,45]. For this reason, features related in the malignant area were analyzed through Doppler ultrasound. The formation and transformation of the tumor vascular network occur through several different morphogenic processes[11,13,16,46,50]. Vascularization is mainly induced by hypoxia[11,13,14,16,46,48] and metabolic and mechanical stimuli[11,13,16,19,31].

The vessels are abnormal from their normal counterparts in relation to organization, structure, and function[11,13,16,46,51]. In the stroma, vessels may be aberrant, numerous, distorted, with insufficient cellular coating, with excess branching, shunts, complex spatial distribution, and anomalous flows[11,13,16,20,31,46]. In addition, they occupy a larger area and vascular perimeter than those in benign mammary neoplasms[31]. Many of these vascular changes were observed through imaging and later assigned to vascularization patterns. The contribution of the network-type vascular pattern (NTVP) predominated over the spot-type vascular pattern (STVP). The NTVP was depicted by detectable flow in numerous distorted and continuous tubular formations with varying diameters, excess branching, and complex spatial distribution. Upon detecting the flow, tubular formations, ramifications, diameter variations, and scattered distribution in the MC stroma were assigned as PVTM.

In our study, the vascular architecture in MC facilitated the comparison of the variations in the hemodynamic's epigastric arteries and provided information about the vascularization formed, which has been confirmed in another study reporting a higher frequency of hemodynamic changes in malignant mammary neoplasias[8]. Furthermore, ultrasonography indicated the vasculogenic activity of the MC because the increased area affected by the ramifications[10,21,31,45,52] and the morphological characteristics of the vessels[11,13,44,45] also increased the shear stress and circumferential tension of the main vascular supply. This fact was evidenced by the flV and IR of the epigastric arteries, in which the NTVP showed greater interference than the STVP in MC. These changes, in relation to the presentation of the stromal vessels in the MC, may be attributed to the adaptation of the wall tonus[5,8-10] of the cranial and caudal epigastric arteries due to increased demand of flow to the malignant mammary neoplasm[11,13,44,45]. Excess branching resulting from the formation of stromal branches, diameter distortions along the pathway[11,13,44,45], alternations in cell coverage, and complex distribution[11,12,14,46] is a characteristic evidenced by MC vascularization imaging, which,

together with the rigidity associated with heterogeneous echotexture, tend to increase the resistance on the flow of the mammary chain affected by MC.

Histological grade[41,43], including heterogeneous echotexture[21,28,43], correlates with greater rigidity. However, it was not possible to conclude whether there was an influence of grade III MC due to the occurrence of only one case. Nevertheless, we observed histological grades I and II and ungraded carcinomas. Low tissue compliance associated with low stromal viscoelasticity due to greater stiffness[28,43] was observed in MCs categorized as grade I, grade II, and ungraded. The increase in shear stress and circumferential tension in the epigastric arteries was reflected in the flV and IR. Reduced viscoelasticity generates extravascular chronic mechanical stress[11,12] and results in stimuli for the formation, remodeling, maintenance, or regression of the vessels that supply tissues[12,17,31] with regard to flow, perfusion, and metabolism[11,12,46]. Consequently, it shapes the hemodynamics of the vessels that irrigate the tissue affected by MC. These findings reinforce the need to evaluate the epigastric arteries for estimating the vascular activity of MC.

In conclusion, MC progression can be investigated based on the hemodynamic evaluation of the cranial and caudal epigastric arteries. In fact, changes are constantly occurring in the stroma, adjacent tissues, and the internal and peripheral vessels of the lesion. Therefore, there is adaptation of the flow and resistance of the blood supply to the affected breasts. Thus, the PSV, EDV, and IR investigated by spectral Doppler, together with the characteristics of the stroma, the presentation of the vessels in the ultrasound image, and the histological grade were characteristics that confirmed the influence of biomechanical forces of the carcinoma on the hemodynamics of the epigastric arteries. Furthermore, increased flow caused by the MC stage and the number of lesions were confirmed by spectral wave evaluation. The results obtained demonstrate part of the biological behavior based on the estimated vascular activity of the

carcinoma and should be extrapolated in the future for the evaluation and indication of adjuvant therapy in dogs.

Conflict of interests

The authors have no conflicts of interest to declare.

REFERENCES

1. Queiroga FL, Raposo T, Carvalho MI, Prada J, Pires I. Canine mammary tumours as a model to study human breast cancer: most recent findings. *In Vivo* 2011;25(3):455-465.
2. Sleeckx N, de Rooster H, Veldhuis Kroeze EJ, Van Ginneken C, Van Brantegem L. Canine mammary tumours, an overview. *Reprod Domest Anim* 2011;46(6):1112-1131.
3. Clemente M, Pérez-Alenza MD, Peña L. Metastasis of canine inflammatory versus non-inflammatory mammary tumours. *J Comp Pathol* 2010;143(2–3):157-163.
4. Diessler ME, Castellano MC, Portiansky EL, Burns S, Idiart JR. Canine mammary carcinomas: influence of histological grade, vascular invasion, proliferation, microvessel density and VEGFR2 expression on lymph node status and survival time. *Vet Comp Oncol* 2017;15(2):450-461.
5. Santos AA, Lopes CC, Ribeiro JR, et al. Identification of prognostic factors in canine mammary malignant tumours: a multivariable survival study. *BMC Vet Res* 2013;9(1):1-11.
6. Perez-Rivas LG, Jerez JM, Fernandez-De Sousa CE, et al. Serum protein levels following surgery in breast cancer patients: A protein microarray approach. *Int J Oncol* 2012;41(6):2200-2206.
7. Santos AA, Matos AJF. Advances in the understanding of the clinically relevant genetic pathways and molecular aspects of canine mammary tumours. Part 2: Invasion, angiogenesis, metastasis and therapy. *Vet J* 2015;205(2):144-153.
8. Davoudi Y, Borhani B, Rad MP, Matin N. The role of Doppler sonography in distinguishing malignant from benign breast lesions. *J Med Ultrasound* 2014;22(2):92-95.
9. Huang YH, Chen JH, Chang YC, et al. Diagnosis of solid breast tumors using vessel analysis in three-dimensional power Doppler ultrasound images. *J Digit Imaging* 2013;26(4):731-739.

10. Yongfeng Z, Ping Z, Wengang L, Yang S, Shuangming T. Application of a novel microvascular imaging technique in breast lesion evaluation. *Ultrasound Med Biol* 2016;42(9):2097-2105.
11. Clegg LE, Mac Gabhann F. Systems biology of the microvasculature. *Integr Biol* 2015;7(5):498-512.
12. Lee GS, Filipovic N, Miele LF, et al. Blood flow shapes intravascular pillar geometry in the chick chorioallantoic membrane. *J Angiogenes. Res* 2010;2:11.
13. Logsdon EA, Finley SD, Popel AS, Mac Gabhann F. A systems biology view of blood vessel growth and remodelling. *J Cell Mol Med* 2014;18(8):1491-1508.
14. Silvestre JS, Smadja DM, Lévy BI. Postischemic revascularization: From cellular and molecular mechanisms to clinical applications. *Physiol Rev* 2013;93(4):1743-1802.
15. Hanahan D, Folkman J. Patterns and emerging mechanisms of the angiogenic switch during tumorigenesis. *Cell* 1996;86(3):353-364.
16. Nagy JA, Chang SH, Shih SC, Dvorak AM, Dvorak HF. Heterogeneity of the tumor vasculature. *Semin Thromb Hemost* 2010;36(3):321–331.
17. Kareva I. Escape from tumor dormancy and time to angiogenic switch as mitigated by tumor-induced stimulation of stroma. *J Theor Biol* 2016;395:11-22.
18. Kim E, Stamatelos S, Cebulla J, Bhujwalla ZM, Popel AS, Pathak AP. Multiscale imaging and computational modeling of blood flow in the tumor vasculature. *Ann Biomed Eng* 2012;40(11):2425-2441.
19. Li S, Meng W, Guan Z, Guo Y, Han X. The hypoxia-related signaling pathways of vasculogenic mimicry in tumor treatment. *Biomed Pharmacother* 2016;80:127-135.
20. Viger L, Denis F, Rosalie M, Letellier C. A cancer model for the angiogenic switch. *J Theor Biol* 2014;360:21-33.

21. Candelaria RP, Hwang L, Bouchard RR, Whitman GJ. Breast ultrasound: current concepts. *Semin Ultrasound CT MR* 2013;34(3):213-225.

22. Gokalp G, Topal U, Kizilkaya E. Power Doppler sonography: anything to add to BI-RADS US in solid breast masses? *Eur J Radiol* 2009;70(1):77-85.

23. Lee WJ, Chu JS, Huang CS, Chang MF, Chang KJ, Chen KM. Breast cancer vascularity: color Doppler sonography and histopathology study. *Breast Cancer Res Treat* 1996;37(3):291-298.

24. Loh ZHK, Allan GS, Nicoll RG, Hunt GB. Ultrasonographic characteristics of soft tissue tumours in dogs. *Aust Vet J* 2009;87(8):323-329.

25. Feliciano MAR, Vicente WRR, Silva MAM. Conventional and Doppler ultrasound for the differentiation of benign and malignant canine mammary tumours. *J Small Anim Pract* 2012;53(6):332-337.

26. Soler M, Dominguez E, Lucas X, et al. Comparison between ultrasonographic findings of benign and malignant canine mammary gland tumours using B-mode, colour Doppler, power Doppler and spectral Doppler. *Res Vet Sci* 2016;107:141-146.

27. Tagawa M, Kanai E, Shimbo G, Kano M, Kayanuma H. Ultrasonographic evaluation of depth-width ratio (D/W) of benign and malignant mammary tumors in dogs. *J Vet Med Sci* 2016;78(3):521-524.

28. Feliciano MAR, Uscategui RAR, Maronezi MC, et al. Ultrasonography methods for predicting malignancy in canine mammary tumors. *PLOS ONE* 2017;12(5):e0178143.

29. Yang WT, Tse GMK, Lam PKW, Metreweli C, Chang J. Correlation between color power Doppler sonographic measurement of breast tumor vasculature and immunohistochemical analysis of microvessel density for the quantitation of angiogenesis. *J Ultrasound Med* 2002;21(11):1227-1235. .

30. Theek B, Opacic T, Möckel D, Schmitz G, Lammers T, Kiessling F. Automated generation of reliable blood velocity parameter maps from contrast-enhanced ultrasound data. Contrast Media Mol. Imaging 2017.

31. Sleeckx N, Van Brantegem L, Van den Eynden G, et al. Lymphangiogenesis in canine mammary tumours: A morphometric and prognostic study. *J Comp Pathol* 2014;150(2–3):184-193.

32. Rutteman G, Withrow S, Macewen E. Tumors of the mammary gland. In: Withrow S, Macewen E, (eds). Small Animal Clinical Oncology. 3rd ed. Philadelphia, PA: WB Saunders; 2001:726-756.

33. Goldschmidt MH, Peña L, Rasotto R, Zappulli V. Classification and grading of canine mammary tumors. *Vet Pathol* 2011;48(1):117-131.

34. Carvalho FC. Ultrassonografia Doppler de linfonodos. In: Carvalho FC, ed. Ultrassonografia Doppler em pequenos animais. Editora Roca., São Paulo; 2009:178-183.

35. Carvalho FC. Ultrassonografia Duplex Doppler vascular: Aspectos Gerais. In: Carvalho FC, ed. Ultrassonografia Doppler em pequenos animais. Editora Roca., São Paulo; 2009:87-97.

36. Sorenmo KU, Rasotto R, Zappulli V, Goldschmidt MH. Development, anatomy, histology, lymphatic drainage, clinical features, and cell differentiation markers of canine mammary gland neoplasms. *Vet Pathol* 2011;48(1):85-97.

37. Gödde R, Kurz H. Structural and biophysical simulation of angiogenesis and vascular remodeling. *Dev Dyn* 2001;220(4):387-401.

38. Mentzer SJ, Konerding MA. Intussusceptive angiogenesis: expansion and remodeling of microvascular networks. *Angiogenesis* 2014;17(3):499-509.

39. Stamatelos SK, Kim E, Pathak AP, Popel AS. A BioImage informatics based reconstruction of breast tumor microvasculature with computational blood flow predictions. *Microvasc Res* 2014;91:8-21.

40. Mori N, Mugikura S, Takahashi S, et al. Quantitative analysis of contrast-enhanced ultrasound imaging in invasive breast cancer: A novel technique to obtain histopathologic information of microvessel density. *Ultrasound Med Biol* 2017;43(3):607-614.

41. Del Cura JL, Elizagaray E, Zabala R, Legórburu A, Grande D. The use of unenhanced Doppler sonography in the evaluation of solid breast lesions. *Am J Roentgenol* 2005;184(6):1788-1794.

42. Chao TC, Lo YF, Chen SC, Chen MF. Color Doppler ultrasound in benign and malignant breast tumors. *Breast Cancer Res Treat* 1999;57(2):193-199.

43. Zhou J, Zhan W, Chang C, et al. Role of acoustic shear wave velocity measurement in characterization of breast lesions. *J Ultrasound Med* 2013;32(2):285-294.

44. Gompper G, Fedosov DA. Modeling microcirculatory blood flow: current state and future perspectives. *Wiley Interdiscip Rev Syst Biol Med* 2016;8(2):157-168.

45. Stanzani D, Chala LF, Barros Nd, Cerri GG, Chammas MC. Can Doppler or contrast-enhanced ultrasound analysis add diagnostically important information about the nature of breast lesions? *Clinics* 2014;69(2):87-92.

46. Auguste P, Lemiere S, Larrieu-Lahargue F, Bikfalvi A. Molecular mechanisms of tumor vascularization. *Crit Rev Oncol Hematol* 2005;54(1):53-61.

47. Chen L, Choyke PL, Wang N, et al. Unsupervised deconvolution of dynamic imaging reveals intratumor vascular heterogeneity and repopulation dynamics. *PLOS ONE* 2014;9(11):e112143.

48. Gilkes DM, Semenza GL. Role of hypoxia-inducible factors in breast cancer metastasis. *Future Oncol* 2013;9(11):1623-1636.

49. Vaupel P, Mayer A. Hypoxia in cancer: significance and impact on clinical outcome. *Cancer Metastasis Rev* 2007;26(2):225-239.

50. Holopainen T, Bry M, Alitalo K, Saaristo A. Perspectives on lymphangiogenesis and angiogenesis in cancer. *J Surg Oncol* 2011;103(6):484-488.

51. Stefanini MO, Qutub AA, Mac Gabhann F, Popel AS. Computational models of VEGF-associated angiogenic processes in cancer. *Math Med Biol* 2012;29(1):85-94.

52. Kwak JY, Kim EK, Kim MJ, Choi SH, Son E, Oh KK. Power Doppler sonography: evaluation of solid breast lesions and correlation with lymph node metastasis. *Clin Imaging* 2008;32(3):167-171.

Table 1. Systolic and diastolic velocities and resistive index of the cranial epigastric artery of the control and mammary neoplasm groups in relation to the categories identified in the mammary neoplasm group.

	Number of female dogs	Peak systolic velocity (cm/s)* (mean ± standard deviation)	End diastolic velocity (cm/s)* (mean ± standard deviation)	Resistive index # [median (range)]
Control group	20	37.18† ± 3.60	11.82† ± 0.89	0.69† (0.59–0.72)
One neoplasm	22	47.55‡‡ ± 9.23	11.78† ± 1.42	0.74‡‡ (0.70–0.83)
Two neoplasms	13	45.77‡‡ ± 7.61	11.40† ± 1.61	0.74‡‡ (0.70–0.83)
Three or more neoplasms	08	44.76†‡‡ ± 11.56	12.35† ± 2.21	0.71†‡‡ (0.67–0.77)
P value		p < 0.01	p > 0.05	p < 0.01
Control group	20	37.18† ± 3.60	11.82† ± 0.89	0.69† (0.59–0.72)
Stage I	15	44.57† ± 6.89	11.54† ± 1.71	0.74‡ (0.70–0.80)
Stage II	21	45.26† ± 8.88	11.65† ± 1.43	0.72‡ (0.67–0.83)
Stage III	07	54.31‡‡ ± 10.97	12.62† ± 1.99	0.75‡ (0.70–0.83)
P value		p < 0.01	p > 0.05	< 0.001
Control group	20	37.18† ± 3.60	11.82† ± 0.89	0.69† (0.59–0.72)
Homogeneous echotexture	06	40.68†‡ ± 3.70	10.83† ± 1.12	0.73‡ (0.70–0.76)
Heterogeneous echotexture	37	47.13‡ ± 9.34	11.98† ± 1.67	0.73‡ (0.67–0.83)
P value		p < 0.01	p > 0.05	p < 0.01
Control group	20	37.20† ± 3.51	11.74† ± 0.93	0.69† (0.59–0.72)
Spot-type vascular pattern	12	44.48‡ ± 5.92	11.78† ± 1.25	0.74‡ (0.70–0.78)
Network-type vascular pattern	30	47.60‡ ± 10.05	11.82† ± 1.79	0.73‡ (0.67–0.83)
P value		p < 0.01	p > 0.05	< 0.001
Control group	20	37.18† ± 3.60	11.82† ± 0.89	0.69† (0.59–0.72)
Carcinoma grade I	30	46.12‡ ± 8.23	11.96† ± 1.66	0.73‡ (0.69–0.83)
Carcinoma grade II	07	53.42‡ ± 8.33	12.00† ± 1.80	0.76‡ (0.71–0.83)
Ungraduated	05	36.68† ± 5.81	10.68† ± 0.86	0.71‡ (0.67–0.74)
P value		p < 0.01	p > 0.05	< 0.001

Different letters indicate difference between groups.

* ANOVA, Tukey's test

Kruskal–Wallis, Dunn's multiple comparison test

Table 2. Systolic and diastolic velocities and resistive index of the caudal epigastric artery of the control and mammary neoplasm groups in relation to the categories identified in the mammary neoplasm group.

	Number of female dogs	Peak systolic velocity (cm/s)* (mean ± standard deviation)	End diastolic velocity (cm/s)* (mean ± standard deviation)	Index of resistivity # [median (range)]
Control group	20	47.12† ± 4.98	12.30† ± 0.82	0.74† (0.71–0.76)
One neoplasm	22	70.36‡ ± 4.96	15.70‡ ± 1.43	0.78‡ (0.73–0.81)
Two neoplasms	13	84.08§ ± 4.07	18.29§ ± 1.91	0.78‡ (0.76–0.82)
Three or more neoplasms	08	90.75¶ ± 3.04	18.55§ ± 1.47	0.79‡ (0.78–0.82)
P value		p < 0.01	p < 0.01	p < 0.01
Control group	20	47.12† ± 4.98	12.30† ± 0.82	0.74† (0.71–0.76)
Stage I	15	76.04‡ ± 9.59	17.59‡ ± 2.17	0.77‡ (0.73–0.79)
Stage II	21	80.78‡ ± 9.06	16.95‡ ± 1.97	0.79‡ (0.77–0.82)
Stage III	07	75.72‡ ± 10.45	15.95‡ ± 2.00	0.79‡ (0.77–0.81)
P value		p < 0.01	p <0.01	< 0.001
Control group	20	47.12† ± 4.98	12.30† ± 0.82	0.71† (0.71–0.76)
Homogeneous echotexture	06	71.46‡ ± 10.66	17.45‡ ± 2.59	0.76‡ (0.73–0.77)
Heterogeneous echotexture	37	79.18‡ ± 9.06	16.96‡ ± 2.03	0.78§ (0.77–0.82)
P value		p < 0.01	p < 0.01	p < 0.01
Control group	20	47.83† ± 5.86	12.51† ± 1.26	0.74† (0.71–0.76)
Spot-type vascular pattern	12	76.75‡ ± 9.59	17.86‡ ± 2.41	0.77‡ (0.76–0.78)
Network-type vascular pattern	30	79.46‡ ± 9.28	16.68‡ ± 1.89	0.79§ (0.77–0.82)
P value		p < 0.01	p < 0.01	< 0.001
Control group	20	47.12† ± 4.98	12.30† ± 0.82	0.74† (0.71–0.76)
Carcinoma grade I	30	76.30‡ ± 9.36	16.82‡ ± 2.15	0.78‡ (0.73–0.82)
Carcinoma grade II	07	81.44‡ ± 9.60	17.65‡ ± 2.25	0.78‡ (0.78–0.79)
Ungraded	05	84.00‡ ± 8.74	17.48‡ ± 1.52	0.79‡ (0.77–0.82)
P value		p < 0.01	p < 0.01	< 0.001

Different letters indicate difference between groups.

* ANOVA, Tukey's test

Kruskal–Wallis, Dunn's Multiple Comparison Test

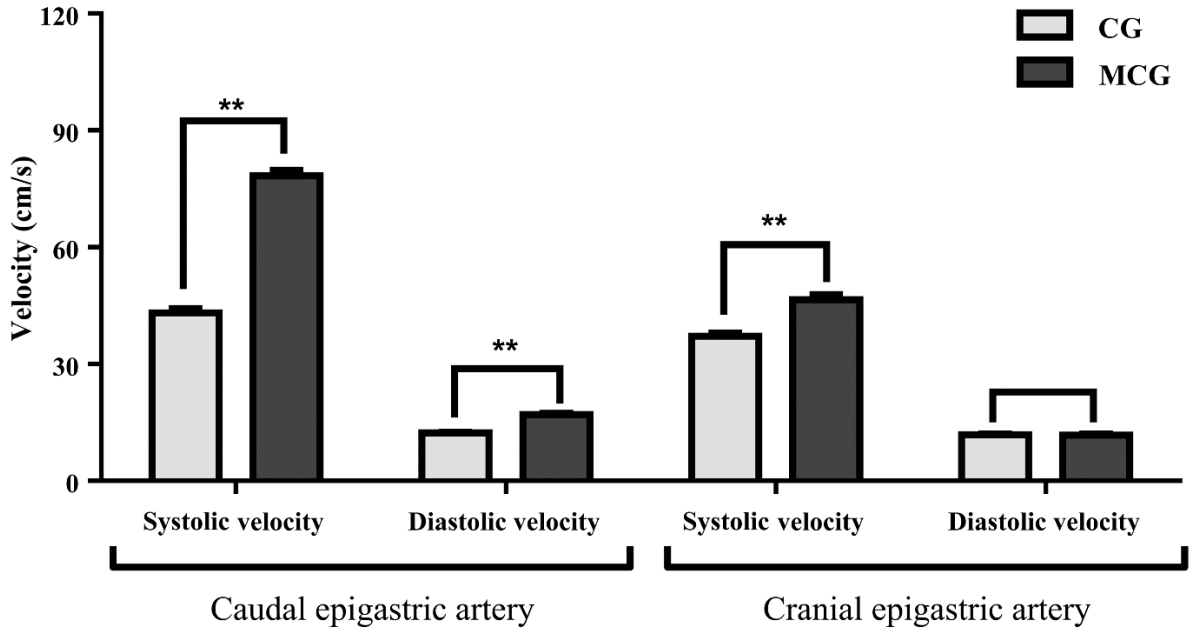

Figure 1. Systolic velocity (PSV) and diastolic velocity (EDV) in the control group (CG) and mammary neoplasm group (MCG). There was significance between the groups in PSV and EDV in the caudal epigastric artery as well as PSV in the cranial epigastric artery ($p < 0.01$). There was no significance between the groups in the EDV in the CrEA ($p > 0.05$). Flow velocities were measured by spectral Doppler. ** Indicates significant difference between groups (ANOVA, Tukey's test).

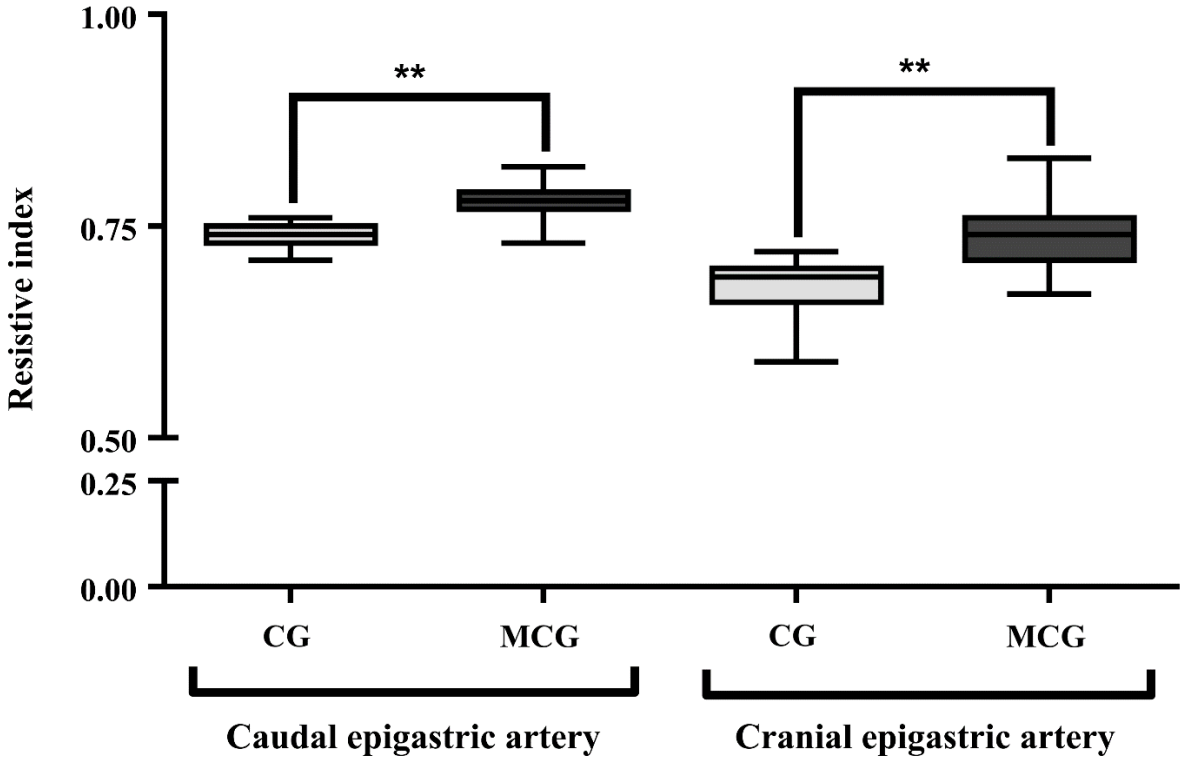

Figure 2. Resistive index (RI) in the control group (CG) and the mammary neoplasm group (MNG). There was significance between the groups in RI in the caudal epigastric artery and the cranial epigastric artery ($p < 0.01$). RI was calculated based on the flow velocities measured by spectral Doppler. ** Indicates significant difference between groups (Kruskal–Wallis, Dunn's multiple comparison test).

3 ARTIGO 2 - DOPPLER ULTRASOUND AS A TOOL FOR DIFFERENTIATION BETWEEN BENIGN AND MALIGNANT CANINE MAMMARY NEOPLASM

Artigo submetido no periódico:

Research in Veterinary Science

Doppler ultrasound as a tool for differentiation between benign and malignant canine mammary neoplasm

Abstract

The aim of the study was to (1) evaluate canine mammary neoplasms using B-mode, color and pulsed Doppler ultrasound and (2) identify factors that could contribute to the interpretation of flow velocities and the resistivity index of neoplasm vessels to differentiate between benign and malignant lesions. In total, 142 mammary neoplasms were examined, and their size, echotexture, flow, vascular distribution, and presentation of vascular pattern in the stroma of the lesions were characterized. In addition, flow velocities and the resistivity index of neoplasm vessels were evaluated. Breasts were surgically removed after clinical staging and ultrasonographic and histopathological examinations, prior to their grouping into glands with benign and malignant mammary neoplasms. Groups formed composed only of initial-stage neoplasms. Vascular dynamics significantly differed between the groups ($p < 0.01$), and flow velocities increased when they presented heterogeneous echotexture, particularly in malignant mammary neoplasms ($p < 0.01$). These findings may confirm some of the peculiarities of carcinomas, including increased vascular and stromal flow and heterogeneity, which have previously been associated with increased stiffness, interstitial pressure, and less viscoelasticity. Further, these peculiarities may alter the hemodynamics of tumor vessels. Thus, the size and echotexture, associated with the hemodynamics of the internal vessels of the mammary neoplasm, may facilitate evaluation of vasculogenesis and show potential as indicators of the biological behavior of neoplasms.

Keywords: neoplasm vascularization; heterogeneous stroma; flow velocities; vascular resistance

1. Introduction

Mammary neoplasms (MNs) are common diseases among female dogs and are the leading cause of death among gynecological malignancies (Sleeckx et al., 2011). Early diagnosis and successful treatment are priorities in promoting patient survival. Thus, the expansion of the understanding of the behavior of mammary neoplasms (MN) may provide an early opportunity for diagnostic and therapeutic interventions because canine MN is an appropriate model for the study of breast cancer (Queiroga et al., 2011). Among the various MN peculiarities, vascularization has been an attractive target for studies on diagnosis and adjuvant therapy (Carmeliet and Jain, 2011).

Reportedly, neoplasm vascularization is predictive of malignancy based on the principle that blood supply is crucial for growth, invasion, proliferation, and formation of metastatic foci (Carmeliet and Jain, 2011; Nagy et al., 2010; Logsdon et al., 2014; Santos and Matos, 2015). Neoplasm vasculogenesis can occur via several distinct mechanisms, which can transform an avascular MN into vascular phenotype under the influence of several neoplasm factors, particularly when cancer cells require a metabolic increase (Auguste et al., 2005; Clegg and Gabhann, 2015; Logsdon et al., 2014; Nagy et al., 2010; Santos and Matos, 2015). However, the blood supply resulting from this neovascularization may involve abnormalities of vessels (Auguste et al., 2005; Nagy et al., 2010; Holopainen et al., 2011).

Benign MNs (BMNs) and malignant MNs (MMNs) present varying degrees of neovascular expansion, with a greater prominence of MMns, which feature a larger number (Yongfeng et al., 2016), area, and perimeter of vessels (Sleeckx et al., 2014); these are factors that highlight a more aggressive behavior (Santos and Matos, 2015; Diessler et al., 2017; Mori et al., 2017) because vascularization has also been associated with histological type and grading (Millanta et al., 2006), higher infiltration, a higher mitotic index, high nuclear grade, absence of necrosis (Queiroga et al., 2011), and hemorrhage (Shivakumar et al., 2009).

Because heterogeneity and increase in the number of vessels are recognized as unfavorable clinical indicators, some studies have already been conducted to characterize neoplasms based on their vascularization and alterations in vascular perfusion (Huang et al., 2013; Feliciano et al., 2017; Theek et al., 2017). Currently, ultrasonography has been indicated for non-invasive vascular description

(Yongfeng et al., 2016; Feliciano et al., 2017; Soler et al., 2016; Theek et al., 2017). In MMNs, imaging findings frequently indicate the presence of vascularization; intense, reverse, or turbulent flow; abnormal vessels with excessive branching and shunts; and complex central and peripheral distribution. In BMNs, flow is usually reduced; therefore, detection may not be possible by Doppler ultrasonography (OK-Chao et al., 1999; Del Cura et al., 2005; Candelaria et al., 2013; Davoudi et al., 2014; Yongfeng et al., 2016). In addition, vascular distribution is mostly peripheral (Sleeckx et al., 2014; Soler et al., 2016).

Influence of the structural and functional abnormalities of blood circulation and neoplasm stroma (Nagy et al., 2010) as biodynamic factors is poorly reported in canine MNs when assessed by ultrasound (Feliciano et al., 2017; Zhou et al., 2013). MNs, while developing, undergo constant proliferation and tissue support (Kareva, 2016). Consequently, they create a heterogeneous environment, which may be associated with greater stiffness and tissue interstitial pressure (Feliciano et al., 2017; Zhou et al., 2013). The primary consequence of stromal transformation is mechanical stress generated in the neoplasm environment (Nagy et al., 2010; Clegg and Gabhann, 2015), with increased shear stress and vascular flow circumferential stress (Auguste et al., 2005; Silvestre et al., 2013; Clegg and Gabhann, 2015; Santos et al., 2016). This causes the presentation and distribution of neoformed vessels to adapt and become more heterogeneous (Clegg and Gabhann, 2015, Restucci, 2000).

Bearing these principles in mind, we aimed to (1) evaluate canine MNs by mode-B, color and pulsed Doppler ultrasound and (2) identify factors that could contribute to the interpretation of flow velocities and the resistivity index (RI) of neoplasm vessels to differentiate between benign and malignant lesions.

2. Material and methods

2.1. Characterization of samples

The study protocol followed the appropriate guidelines and was approved by the Ethics Committee on Animal Use of the University of Passo Fundo (CEUA-UPF), in the city of Passo Fundo, State of Rio Grande do Sul, Brazil, registered under the number 030/2017; further, the study was conducted in support of the Law no. 24.645 of 07/10/1934 art. 64 (Criminal Offenses Act), Law No.

11,794 of 10/8/2008, which establishes procedures for the scientific use of animals (Law on Environmental Crimes), and Law no. 9.605, of 12/02/98, art. 32, in accordance with the Ethical Principles for the Use of Laboratory Animals of the Brazilian Society of Science in Laboratory Animals. In total, MNs of 82 unspayed female dogs were evaluated at the Veterinary Hospital of the University of Passo Fundo (HV-UPF). Female dogs were selected based on oncologic staging, using the version adapted by Rutteman et al. (2001) for epithelial neoplasms. Thus, neoplasm size (T) was categorized into T1 (<3 cm), T2 (between 3 and 5 cm), and T3 (>5 cm); involvement of regional lymph nodes (N) as N0 (absent) and N1 (local metastasis); and distant metastasis (M) as M0 (absent) and M1 (present). Among these, stages 1 (T1, N0, and M0), 2 (T2, N0, and M0), 3 (T3, N0, and M0), 4 (any T, N1, and M0), and 5 (any T, any N, and M1) were defined. Criteria for inclusion were based on stages 1, 2, and 3 and the absence of inflammatory disease, estrus, and skin lesions. Mammary and regional lymph nodes were removed and submitted for histopathological examination. After surgical excision, tissues were fixed in 10% formaldehyde and subsequently embedded in paraffin. Histological sections (5 μm thick) were obtained and stained with hematoxylin and eosin. Neoplasia classification was performed according to Goldschmidt et al. (2011), by the Laboratory of Animal Pathology of HV-UPF.

2.2. Ultrasonographic study

After clinical evaluation and prior to surgical procedure, MNs and regional lymph nodes were examined with a 4–13-MHz linear transducer (Mylab 70, Esaote, Genova, Italy). The dogs were examined in the dorsal recumbence, and no chemical restraint was required. In order to reduce subjectivity all examinations were performed by the same operator. While evaluating MNs, the size (T1, T2, and T3), echotexture (homogeneous or heterogeneous) in B-mode, presence or absence of flow and presentation of vascular patterns on color Doppler were verified. In vasculature distribution, flow was observed to be present in the periphery and inside the tumor, being categorized into peripheral (PVD) when vessels were found only in the periphery of the lesion, internal (IVD) when they were found only within the stroma, and mixed (MVD) in cases where both peripheral and internal vessels were evidenced. Based on the identification of flow and vascular distribution, it was possible to verify the formation, morphology, and vascular distribution. Based on these characteristics, two vascular patterns

(VPs) in the tumor stroma were proposed: (1) the mesh vascular pattern (MVP) applies to continuous, numerous, distorted tubular formations with varied diameters, excessive branching, and complex spatial distribution (Figure 1) and (2) the spot vascular pattern (SVP) applies to tubular, branched formations, with variable diameters and a dispersed spatial distribution (Figure 1). In the evaluation of axillary and inguinal lymph nodes, round shape, narrow or absent hilum, hypoechogenicity of the parenchyma, sharp margins, presence of posterior acoustic enhancement, and blood flow with peripheral or complex distribution were used as exclusion criteria; these images are related to lymphatic involvement (Carvalho, 2009a). Examination of the tumor vessels were initiated in B-mode, obtaining images in the longitudinal and transversal planes, observing the wall thickness, luminal content, diameter, and vessel's reaction to the transducer's mechanical pressure, when possible. Later, color Doppler was used to evaluate the presence, direction, and characteristics of the flow, thereby confirming luminal viability. Spectral wave analysis was performed using pulsed Doppler, maintaining insonation angle (θ) < 60°, and sample volume was adjusted to the vessel diameter. Pulse gain and pulse repetition frequency were refined according to flow velocity (Vfl), spectral wave morphology, peak systolic velocity (PSV), end diastolic velocity (EDV), and resistivity index (RI; RI = PSV − EDV) / PSV) (Carvalho, 2009b). The aforementioned analyses were performed in three times each, using the median of each value for this study, and the images were digitally stored for analysis.

2.3. Statistical analysis

Quantitative variables were tested for their normality using the Kolmogorov–Smirnov test. All variables obtained (PSV, EDV, and RI), regardless of whether they belonged to the categories related to benign or malignant neoplasm (size, histological grade, echotexture, and vascular distribution), were found not to be normally distributed after being analyzed by Mann–Whitney *U*-test or Kruskal–Wallis test, followed by Dunn's *post-hoc* multiple-comparison test. Qualitative variables were organized in contingency tables, and the relative and/or absolute frequencies were obtained from descriptive statistics. A likelihood ratio test was used in 3 × 2 tables to verify the association between categorical variables, whereas Fisher's exact test was used in 2 × 2 tables because in both types of tables, the

expected frequencies were <5. The data were considered significantly different with a probability of <5% ($p < 0.05$).

3. Results

3.1. Characterization of breast neoplasm

In total, 142 neoplasms were evaluated in 82 canine females (aged 3–15 years). Notably, no vascular flow was detected on color Doppler in 5 benign neoplasms (mean size, 1.2 cm) and one malignant neoplasm (size, 1.0 cm). Thus, the benign mammary neoplasm group (BMNG) comprised 36 vascularized breast neoplasm on color Doppler, with a histopathological diagnosis of BMN. The group included cases of simple adenoma (8/36), ductal adenoma (6/36), complex adenoma (8/36), and mixed benign tumors (14/36). Ultrasound examination of the BMNG revealed neoplasms <3.0 cm in size (36/36); a predominance of homogeneous echotexture (26/36), with fewer cases of heterogeneous echotexture (10/36); and a higher occurrence of MVD (18/36), followed by mixed distribution (13/36) and, less frequently, IVD (5/36), with half of the BMNG presenting SVP (18/36). The malignant mammary neoplasm group comprised 100 vascularized neoplasms on color Doppler with a histopathological diagnosis of MMN. The malignant mammary neoplasm group (MMNG) comprised cases of simple carcinoma (44/100), complex tumors (28/100), solid tumors (5/100), mixed tumors (10/100), adenosquamous tumors (9/100), and carcinosarcoma (4/100). Ultrasound examination of the MMNG revealed 47% of neoplasms <3.0 cm in size (47/100), 43% between 3.0 and 5.0 cm (43/100) and 10% of neoplasms >5.0 cm (10/100). In addition, it was possible to observe a higher incidence of heterogeneous echotexture (77/100), compared with homogeneous echotexture (23/100), and a higher occurrence of MVD (67/100), followed by PVD (30/100) and, less frequently, IVD (3/36). The vessels in the neoplasm stroma presented a lower incidence of SVP (18/100) than of MVP (52/100). However, it was not possible to classify the presentation of the peripheral vessels in 50% of BMNs (18/36) and 30% of MMNs (30/100) as there was no variation in the presentation characteristics. From these characteristics, it was possible to observe a significant difference ($p < 0.01$) between BMNG and MMNG while comparing the neoplasm size, echotexture, vascular distribution, and presentation of

vascular pattern (Table 1). Supported by the histopathological criteria of malignancy, the neoplasm of MMNG were graded and distributed. Grade I carcinoma was the most frequent neoplasm (72/100), followed by grade II (21/100), grade III (2/100), and non-graded neoplasms (5/100). Notably, there was no significant difference between them while comparing Vfl and RI (Table 2).

3.2. Ultrasonography of neoplasm vascularization

Vascular flow in all 36 BMNs and 100 MMNs was identified by color Doppler, and the spectral graph was plotted by pulsed Doppler for the same neoplasms. From the identification of the arterial spectral wave morphology, PSV and EDV made it possible to analyze RI in both groups (Table 2). BMNs had lower PSV, EDV, and RI and demonstrated a statistically significant difference ($p < 0.01$) when compared with MMNs. In the search for a relation among spectral wave variations, BMNs were categorized according to the echotexture, vascular distribution, and presentation of vascular pattern, whereas MMNs were categorized according to size, histological grade, echotexture, vascular distribution, and presentation of vascular pattern. Histological classification showed no significant differences among grades I, II, III, and non-graded tumors ($p > 0.05$); however, neoplasm size exhibited a significant difference ($p < 0.01$). In MMNs >3.0 cm in size, PSV, EDV, and RI were larger compared with neoplasms <3.0 cm. Echotexture of the BMN parenchyma appears to interfere with the spectral waves because when echotexture was heterogeneous, the Vfl values were higher than when the echotexture was homogeneous ($p < 0.01$), but it was not higher enough to cause greater resistance ($p > 0.05$). By contrast, in MMNs, heterogeneous echotexture showed greater Vfl and RI than homogeneous echotexture ($p < 0.01$). Stromal MVD showed higher Vfl values compared with PVD and IVD in BMNs ($p < 0.01$) and no difference in terms of RI ($p > 0.05$). However, in MMNs, there was no difference in terms of Vfl between MVD and IVD ($p > 0.05$), but MVD was higher than PVD ($p < 0.01$). There was no significant difference in terms of RI between IVD and MVD ($p > 0.05$), but their RI were significantly different from that in PVD ($p < 0.01$). PSV, EDV, and RI in SVP and in the absence of vessels in BMN stroma were not significantly different ($p > 0.05$), but they were higher when SVP and MVP occurred in MMN than when peripheral vessels were observed ($p < 0.01$).

4. Discussion

Canine MNs, common oncological diseases in female dogs, are associated with the practice of early ovariohysterectomy (Diessler et al., 2017). In our study, large numbers of BMNs and MMNs were found during the histopathological examination of neoplasm in mammary glands of female dogs, with a mean age of 10 years (28.9% and 71.1%, respectively). The characteristics of the affected population in our study agree with other studies, but they disagree with the average proportion of 50% for MMNs (Ferreira et al., 2009; Sleeckx et al., 2011).

Ultrasonography was a concise method for detecting neoplasm vascularization and characterizing vessels, as previously demonstrated in other studies (Kwak et al., 2008; Feliciano et al., 2012; Candelaria et al., 2013; Davoudi et al., 2014). Therefore, it can be considered an important auxiliary tool in the predictive characterization of malignancy (Davoudi et al., 2014; Feliciano et al., 2017). BMNs and MMNs show different levels of vascular development (Yongfeng et al., 2016), with malignancies being generally hypervascularized and displaying an enhanced flow signal on color Doppler, in contrast with benign lesions (Soler et al., 2016). In MMNs, the peritumoral and internal region have higher density and greater area and vessel perimeter (Sleeckx et al., 2014), as seen in our study from vascular distribution and presentation, suggesting a strong relationship between vascularization and neoplasm biological behavior, since the vascular increase in MMNs was associated with the histological grade (Millanta et al., 2006), infiltrative growth, mitotic index, and nuclear grade (Queiroga et al., 2011).

Neoplasm size in canine mammary carcinomas may suggest the differentiation between benign and malignant neoplasm because larger MNs (T3) were diagnosed as malignant and presented (among several other characteristics) a higher proliferation rate, as observed using immunohistochemical markers (Ferreira et al., 2009). Similarly, there is a positive association between neoplasm aggressiveness and greater flux intensity in smaller MNs (T1) (Lee et al., 2010; Huang et al., 2013; Soler et al., 2016). Therefore, factors such as vascularization should be used because changes in neoplasm perfusion occur even before changes in size can be seen (Stanzani et al., 2014) through mechanisms that allow the transformation of an avascular lesion into a vascular phenotype (Auguste et al., 2005). In our study, no flow could be seen in six nodules on color Doppler because they had small size (T1); only one

of them had a diagnosis of MMN, whereas five were diagnosed as BMNs. These results corroborate our findings regarding flow in neoplasm because the other BMNs presented flow in their stroma less frequently than smaller MMNs (T1) (Lee et al., 2010; Huang et al., 2013; Soler et al., 2016). The absence of internal flow in the group of small MNs may be related to the state of dormancy that some neoplasm manifest, which is supported by phenomena that include lack of stimuli and presence of factors inhibiting vascular activity (Kareva, 2016).

The observed flow velocities followed neoplasm size being increased in larger neoplasm (T2 and T3), possibly due to the higher metabolic demand of the growing stroma (Auguste et al., 2005; Kim et al., 2012; Logsdon et al., 2014; Kareva, 2016), which was in disagreement with the positive association found between neoplasm aggressiveness and increased neoplasm flow velocity in T1 (Lee et al., 2010). RI was similarly higher in T2 and T3 MMNs, which can possibly be attributed to the stromal development, which becomes stiffer and less viscoelastic as it expands and gathers collagen deposits, formations of fibrotic foci, greater cell density, and a higher proportion of interstitial fluids, proteins, and blood cells (Zhou et al., 2013; Feliciano et al., 2017). Histological grade has also been correlated with greater stromal rigidity (Zhou et al., 2013), an important factor in vascular hemodynamics. However, we did not observe any influence of histological grade on Vfl and RI in grade I, II, and III MMNs, as observed in relation to size.

Another important characteristic, which can be interpreted along with vascularization, was the variation of stroma in ultrasound images because MNs jointly adapt their tissues and vascularization during their evolution (Clemente et al., 2010; Diessler et al., 2017). Although occurring to a greater extent in MMNs, heterogeneity alone cannot be considered a unique feature of malignancy. However, when stroma was used to explain flow variations, it was shown to be determinant because the lower perfusion in the developing tissue generates reactions and supports in the neoplasm environment (Feliciano et al., 2017; Logsdon et al., 2014; Soler et al., 2016; Stamatelos et al., 2014; Theek et al., 2017; Zhou et al., 2013), which can influence vascular dynamics (Davoudi et al., 2014; Huang et al., 2013; Yongfeng et al., 2016); it could be observed in BMN and MMN vessels, based on the evaluation of Vfl, which presented differences in terms of relation to homogeneous and heterogeneous echotexture. However, the particularity that made it possible to differentiate BMNs from MMNs was RI, which was

different only in the heterogeneous malignant tumors and signaled a greater resistance, as previously reported in other studies, due to the rigid stroma resulting from reactions and supports common in MMNs (Feliciano et al., 2017; Zhou et al., 2013).

Benign and malignant MNs have different degrees of vascular growth (Yongfeng et al., 2016), and malignant neoplasm have a wider vascular distribution (Kwak et al., 2008, Candelaria et al., 2013; Sleeckx et al., 2014; Stanzani et al., 2014; Yongfeng et al., 2016) and a larger area and perimeter than benign ones (Sleeckx et al., 2014). A wide vascular distribution was observed in MNs, particularly in MMNs with the highest proportion of MVD. In addition, the Vfl values were also higher in BMN and MMN cases with MVD compared with IVD or PVD cases, and these results are possibly associated with increased flow (Soler et al., 2016). By contrast, RI was not significantly different between IVD and MVD cases and appeared to withstand greater resistance when compared with MMN cases with PVD, as they showed no difference in BMNs. These results confirm that mammary carcinomas are stiffer than benign neoplasm (Feliciano et al., 2017; Zhou et al., 2013), and this condition is possibly related to RI.

The heterogeneity of the formed and remodeled vessels (Logsdon et al., 2014; Clegg and Gabhann, 2015; Nagy et al., 2010; Santos and Matos, 2015) can influence vascularization activity (Lee et al., 2010; Stamatelos et al., 2014; Theek et al., 2017) via formation, maintenance, or regression stimuli during growth and tissue support. This occurs to supply blood to areas of metabolic insufficiency, hypoxia, ischemia, and necrosis in a heterogeneous stroma. Such areas have already been associated with high demand from cancer cells (Aguste et al., 2005) and are aberrant, numerous, tortuous, with little coating, overbranching, and a complex spatial distribution, and may also have anomalous flows and greater permeability (Kim et al., 2012; Nagy et al., 2010; Stanzani et al., 2014), characteristics that could be identified in a large part of the lesions on image examination and helped us classify VPs.

Once the structural and organizational presentations of vascularization have been divided according to color Doppler into MVP and SVP from IVD and MVD cases, we could verify the low influence of the heterogeneity of vascular components in MNs. These factors helped us interpret the hemodynamic variations of blood flow as having a greater contribution from extravascular biomechanics, i.e., from the stroma. This alternation between BMN and MMN may have occurred due to increased shear and circumferential stresses (Logsdon et al., 2014; Stanzani et al., 2014; Clegg and

Gabhann, 2015; Gompper and Fedoson, 2016) on the numerous, tortuous, excessively branched vascular pathways with complex distribution, as observed in our study, wherein Vfl and RI were higher in MMNs with SVP and MVP, compared with the absence of vessels inside the tumor, demonstrating that extravascular action has a strong influence on flow dynamics, possibly associated with the effects of the heterogeneous echotexture of the stroma, which occurred more frequently in MMNs.

5. Conclusion

The increased flow velocities and the RI in breast neoplasms were associated with more aggressive neoplasm behavior, and these factors should be studied and correlated to patient prognosis and survival. In benign and malignant neoplasms, the observed vascularization on color Doppler and flow dynamics from the spectral waves was interesting when different neoplasm size, echotextures, vascular distributions, and presentation of VPs were compared, as the formed circulation constitutes the main path for imaging agents and drug in MNs. In addition, echotexture was shown to directly interfere in the flow, an important fact in the interpretation of the findings, due to its association with high extravascular and intratumoral pressure, as a consequence of higher resistance in MMNs. Thus, when neoplasm vascularization and stromal characteristics are associated, they become attractive diagnostic and therapeutic targets. Evaluation of vascular activity is also of potential relevance in the identification of antiangiogenic adjuvant therapies in initial-stage MNs in canines.

Acknowledgements

The authors would like to thank the Graduate Program in Veterinary Medicine of the Universidade Federal de Santa Maria and the Veterinary Medicine Course of Universidade de Passo Fundo for providing technical support.

Funding

This research did not receive any specific grant from funding agencies in the public, commercial, or not-for-profit sectors.

References

Auguste, P., Lemiere, S., Larrieu-Lahargue, F., Bikfalvi, A., 2005. Molecular mechanisms of tumor vascularization. Crit. Rev. Oncol. Hematol. 54, 53–61. https://doi.org/10.1016/j.critrevonc.2004.11.006

Candelaria, R.P., Hwang, L., Bouchard, R.R., Whitman, G.J., 2013. Breast Ultrasound: Current Concepts. Semin Ultrasound CT MRI 34, 213–225. https://doi.org/10.1053/j.sult.2012.11.013

Carmeliet, P., Jain, R.K., 2011. Molecular mechanisms and clinical applications of angiogenesis. Nature 473, 298–307. https://doi.org/10.1038/nature10144

Carvalho, F.C., 2009a. Doppler ultrasonography of lymph nodes, in: Carvalho, F. C., Doppler Ultrasonography in small animals. Publisher: Roca., São Paulo, pp. 178–183.

Carvalho 2009b. Vascular Doppler Ultrasonography: General Aspects, in: Carvalho, F. C., Doppler Ultrasonography in small animals. Publisher: Roca., São Paulo, pp. 87-97.

Clegg, L.E., Mac Gabhann, F., 2015. Systems biology of the microvasculature. Integr. Biol. 7, 498–512. https://doi.org/10.1039/C4IB00296B

Clemente, M., Pérez-Alenza, M.D., Illera, J.C., Peña, L., 2010. Histological, immunohistological, and ultrastructural description of vasculogenic mimicry in canine mammary cancer. Vet. Pathol. 47, 265–274. https://doi.org/10.1177/0300985809353167

Davoudi, Y., Borhani, B., Rad, M.P., Matin, N., 2014. The role of doppler sonography in distinguishing malignant from benign breast lesions. J. Med. Ultrasound 22, 92–95. https://doi.org/10.1016/j.jmu.2013.12.001

Del Cura, J.L., Elizagaray, E., Zabala, R., Legórburu, A., Grande, D., 2005. The use of unenhanced doppler sonography in the evaluation of solid breast lesions. AJR Am. J. Roentgenol. 184, 1788–1794. https://doi.org/10.2214/ajr.184.6.01841788

Diessler, M.E., Castellano, M.C., Portiansky, E.L., Burns, S., Idiart, J.R., 2017. Canine mammary carcinomas: influence of histological grade, vascular invasion, proliferation, microvessel density and VEGFR2 expression on lymph node status and survival time. Vet. Comp. Oncol. 15, 450–461. https://doi.org/10.1111/vco.12189

Feliciano, M.A.R., Uscategui, R.A.R., Maronezi, M.C., Simões, A.P.R., Silva, P., Gasser, B., Pavan, L.,

Carvalho, C.F., Canola, J.C., Vicente, W.R.R., 2017. Ultrasonography methods for predicting malignancy in canine mammary tumors. PLoS One 12, 1–15. https://doi.org/10.1371/journal.pone.0178143

Feliciano, M.A.R., Vicente, W.R.R., Silva, M.A.M., 2012. Conventional and Doppler ultrasound for the differentiation of benign and malignant canine mammary tumours. J. Small Anim. Pract. 53, 332–337. https://doi.org/10.1111/j.1748-5827.2012.01227.x

Ferreira, E., Bertagnolli, A.C., Cavalcanti, M.F., Schmitt, F.C., Cassali, G.D., 2009. The relationship between tumour size and expression of prognostic markers in benign and malignant canine mammary tumours. Vet. Comp. Oncol. 7, 230–235. https://doi.org/10.1111/j.1476-5829.2009.00193.x

Goldschmidt, M.H., Peña, L., Rasotto, R., Zappulli, V., 2011. Classification and grading of canine mammary tumors. Vet. Pathol. 48, 117–131. https://doi.org/10.1177/0300985810393258

Gompper, G., Fedosov, D.A., 2016. Modeling microcirculatory blood flow: Current state and future perspectives. Wiley Interdiscip. Rev. Syst. Biol. Med. 8, 157–168. https://doi.org/10.1002/wsbm.1326

Holopainen, T., Bry, M., Alitalo, K., Saaristo, A., 2011. Perspectives on lymphangiogenesis and angiogenesis in cancer. J. Surg. Oncol. 103, 484–488. https://doi.org/10.1002/jso.21808

Huang, Y.H., Chen, J.H., Chang, Y.C., Huang, C.S., Moon, W.K., Kuo, W.J., Lai, K.J., Chang, R.F., 2013. Diagnosis of Solid Breast Tumors Using Vessel Analysis in Three-Dimensional Power Doppler Ultrasound Images. J. Digit. Imaging 26, 731–739. https://doi.org/10.1007/s10278-012-9556-5

Kareva, I., 2016. Escape from tumor dormancy and time to angiogenic switch as mitigated by tumor-induced stimulation of stroma. J. Theor. Biol. 395, 11–22. https://doi.org/10.1016/j.jtbi.2016.01.024

Kim, E., Stamatelos, S., Cebulla, J., Bhujwalla, Z.M., Popel, A.S., Pathak, A.P., 2012. Multiscale imaging and computational modeling of blood flow in the tumor vasculature. Ann. Biomed. Eng. 40, 2425–2441. https://doi.org/10.1007/s10439-012-0585-5

Kwak, J.Y., Kim, E.K., Kim, M.J., Choi, S.H., Son, E., Oh, K.K., 2008. Power Doppler sonography:

evaluation of solid breast lesions and correlation with lymph node metastasis. Clin. Imaging 32, 167–171. https://doi.org/10.1016/j.clinimag.2007.12.004

Lee, G.S., Filipovic, N., Miele, L.F., Lin, M., Simpson, D.C., Giney, B., Konerding, M.A., Tsuda, A., Mentzer, S.J., 2010. Blood flow shapes intravascular pillar geometry in the chick chorioallantoic membrane. J. Angiogenes. Res. 2, 1–9. https://doi.org/10.1186/2040-2384-2-11

Logsdon, E.A., Finley, S.D., Popel, A.S., MacGabhann, F., 2014. A systems biology view of blood vessel growth and remodelling. J. Cell. Mol. Med. 18, 1491–1508. https://doi.org/10.1111/jcmm.12164

Millanta, F., Silvestri, G., Vaselli, C., Citi, S., Pisani, G., Lorenzi, D., Poli, A., 2006. The role of vascular endothelial growth factor and its receptor Flk-1 / KDR in promoting tumour angiogenesis in feline and canine mammary carcinomas: A preliminary study of autocrine and paracrine loops. Res Vet Sci. 81, 350–357. https://doi.org/10.1016/j.rvsc.2006.01.007

Mori, N., Mugikura, S., Takahashi, S., Ito, K., Takasawa, C., Li, L., Miyashita, M., Kasajima, A., Mori, Y., Ishida, T., Kodama, T., Takase, K., 2017. Quantitative analysis of contrast-enhanced ultrasound imaging in invasive breast cancer: A novel technique to obtain histopathologic information of microvessel density. Ultrasound Med. Biol. 43, 607–614. https://doi.org/10.1016/j.ultrasmedbio.2016.11.009

Nagy, J.A., Chang, S.H., Shih, S.C., Dvorak, A.M., Dvorak, H.F., 2010. Heterogeneity of the tumor vasculature. Semin. Thromb. Hemost. 36, 321–331. https://doi.org/10.1055/s-0030-1253454

OK-Chao, T.C., Lo, Y.F., Chen, S.C., Chen, M.F., 1999. Color Doppler ultrasound in benign and malignant breast tumors. Breast Cancer Res. Treat. 57, 193–199. https://doi.org/10.1023/A:1006277617884

Queiroga, F.L., Raposo, T., Carvalho, M.I., Prada, J., Pires, I., 2011. Canine mammary tumours as a model to study human breast cancer: most recent findings. In Vivo 25, 455–465.

Restucci, B., 2000. Evaluation of angiogenesis in canine mammary tumors by quantitative platelet endothelial cell adhesion molecule immunohistochemistry. Vet. Pathol. 37, 297–301. https://doi.org/10.1354/vp.37-4-297

Rutteman, G., Withrow, S., Macewen, E., 2001. Tumors of the mammary gland, in: Withrow, S.;

Macewen, E., Small Animal Clinical Oncology. 3. ed. WB Saunders, Philadelphia, pp. 726-756.

Santos, A., Lopes, C., Gärtner, F., Matos, A.J.F., 2016. VEGFR-2 expression in malignant tumours of the canine mammary gland: a prospective survival study. Vet. Comp. Oncol. 14, e83–e92. https://doi.org/10.1111/vco.12107

Santos, A.A., Matos, A.J.F., 2015. Advances in the understanding of the clinically relevant genetic pathways and molecular aspects of canine mammary tumours. Part 2: Invasion, angiogenesis, metastasis and therapy. Vet. J. 205, 144–153. https://doi.org/10.1016/j.tvjl.2015.03.029

Shivakumar, S., Prabhakar, B.T., Jayashree, K., Rajan, M.G.R., Salimath, B.P., 2009. Evaluation of serum vascular endothelial growth factor (VEGF) and microvessel density (MVD) as prognostic indicators in carcinoma breast. J. Cancer Res. Clin. Oncol. 135, 627–636. https://doi.org/10.1007/s00432-008-0497-9

Silvestre, J.-S., Smadja, D.M., Levy, B.I., 2013. Postischemic Revascularization: From Cellular and Molecular Mechanisms to Clinical Applications. Physiol. Rev. 93, 1743–1802. https://doi.org/10.1152/physrev.00006.2013

Sleeckx, N., de Rooster, H., Veldhuis Kroeze, E., Van Ginneken, C., Van Brantegem, L., 2011. Canine Mammary Tumours, an Overview. Reprod. Domest. Anim. 46, 1112–1131. https://doi.org/10.1111/j.1439-0531.2011.01816.x

Sleeckx, N., Van Brantegem, L., Van den Eynden, G., Fransen, E., Casteleyn, C., Van Cruchten, S., Veldhuis Kroeze, E., Van Ginneken, C., 2014. Lymphangiogenesis in canine mammary tumours: A morphometric and prognostic study. J. Comp. Pathol. 150, 184–193. https://doi.org/10.1016/j.jcpa.2013.09.006

Soler, M., Dominguez, E., Lucas, X., Novellas, R., Gomes-Coelho, K.V., Espada, Y., Agut, A., 2016. Comparison between ultrasonographic findings of benign and malignant canine mammary gland tumours using B-mode, colour Doppler, power Doppler and spectral Doppler. Res. Vet. Sci. 107, 141–146. https://doi.org/10.1016/j.rvsc.2016.05.015

Stamatelos, S.K., Kim, E., Pathak, A.P., Popel, A.S., 2014. A bioimage informatics based reconstruction of breast tumor microvasculature with computational blood flow predictions. Microvasc. Res. 91, 8–21. https://doi.org/10.1016/j.mvr.2013.12.003

Stanzani, D., Chala, L., Barros, N., Cerri, G., Chammas, M., 2014. Can Doppler or contrast-enhanced ultrasound analysis add diagnostically important information about the nature of breast lesions? Clinics 69, 87–92. https://doi.org/10.6061/clinics/2014(02)03

Theek, B., Opacic, T., Möckel, D., Schmitz, G., Lammers, T., Kiessling, F., 2017. Automated generation of reliable blood velocity parameter maps from contrast-enhanced ultrasound data. Contrast Media Mol. Imaging 2017. https://doi.org/10.1155/2017/2098324

Yongfeng, Z., Ping, Z., Wengang, L., Yang, S., Shuangming, T., 2016. Application of a novel microvascular imaging technique in breast lesion evaluation. Ultrasound Med. Biol. 42, 2097–2105. https://doi.org/10.1016/j.ultrasmedbio.2016.05.010

Zhou, J., Zhan, W., Chang, C., Zhang, J., Yang, Z., Dong, Y., Zhou, C., Song, Y., 2013. Role of Acoustic Shear Wave Velocity Measurement in Characterization of Breast Lesions. J. Ultrasound Med. 32, 285–294.

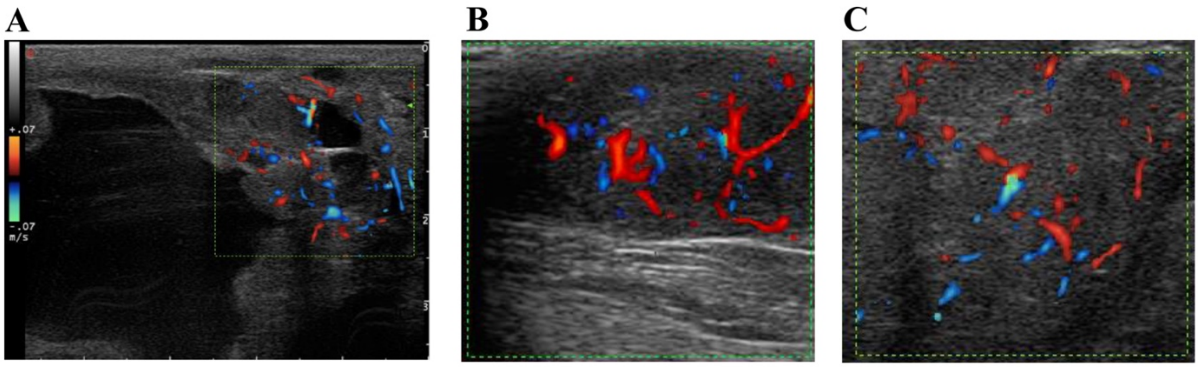

Figure 1. Mammary neoplasm presenting vascular flow with mixed distribution (A). Mesh vascular pattern presenting numerous distorted tubular formations with varied diameters, excessive branching, and complex spatial distribution (B). Spot vascular pattern presenting tubular, branched formations, with variations in diameter and dispersed spatial distribution (C).

Table 1. Characterization of mammary neoplasms in female dogs by ultrasonographic examination, according to histopathological diagnoses of benign or malignant mammary neoplasms

Variables		Neoplasm type				P-value
		Benign		Malignant		
		N	%	n	%	
Neoplasm size	<3.0 cm	36	100.0	47	47.0	<0.01*
	3.0–5.0 cm	0	0.0	43	43.0	
	>5.0 cm	0	0.0	10	10.0	
Echotexture	Homogeneous	26	72.2	23	23.0	<0.01[a]
	Heterogeneous	10	27.8	77	77.0	
Vessel distribution	Peripheral	18	50.0	30	30.0	<0.01*
	Internal	5	13.9	03	3.0	
	Mixed	13	36.1	67	67.0	
Vascular pattern	Absent	18	50.0	30	30.0	<0.01*
	Spot	18	50.0	18	18.0	
	Mesh	0	0.0	52	52.0	

* Probability < 5% ($p < 0.05$) indicates a significant difference (likelihood ratio test).

[a] Fisher's exact test was applied to 2 × 2 tables when estimated counts were <5.

Table 2. Peak systolic and end diastolic velocities and resistivity index (median, minimal, and maximum) of peripheral, internal, and mixed vessels in benign and malignant mammary neoplasms, according to ultrasound findings

	Number of neoplasm	Peak systolic velocity (cm/s)	End diastolic velocity (cm/s)	Resistivity index
Neoplasm type				
Benign	36	37.3^{A} (26.3–41.3)	10.2^{A} (8.3–12.5)	0.71^{A} (0.68–0.74)
Malignant	100	59.4^{B} (36.2–62.9)	14.1^{B} (10.4–18.0)	0.74^{B} (0.68–0.77)
Neoplasm size				
Malignant				
< 3.0 cm	47	45.8^{a} (36.2–62.2)	12.7^{a} (10.4–16.5)	0.73^{a} (0.68–0.76)
3.0 – 5.0 cm	43	60.5^{b} (42.3–62.9)	14.7^{b} (11.0–18.0)	0.76^{b} (0.70–0.77)
> 5.0 cm	10	61.2^{b} (58.7–62.4)	14.8^{b} (14.0–16.2)	0.76^{b} (0.74–0.77)
Histological grade				
Grade 1	72	58.5^{a} (36.2–62.9)	14.2^{a} (10.4–18.0)	0.74^{a} (0.68–0.77)
Grade 2	21	60.2^{a} (41.4–62.4)	14.6^{a} (10.9–16.9)	0.74^{a} (0.72–0.76)
Grade 3	2	61.3^{a} (61.2–61.4)	16.3^{a} (15.3–17.2)	0.74^{a} (0.72–0.75)
Non–graded	5	50.9^{a} (42.4–61.3)	13.2^{a} (12.5–14.7)	0.74^{a} (0.70–0.76)
Echotexture				
Benign				
Homogeneous	26	32.7^{A} (26.3–41.3)	9.9^{A} (8.3–11.3)	0.71^{A} (0.68–0.74)
Heterogeneous	10	39.9^{B} (35.8–40.4)	11.2^{B} (10.0–12.5)	0.72^{A} (0.69–0.73)
Malignant				
Homogeneous	23	42.1^{A} (36.3–60.4)	11.6^{A} (10.4–15.6)	0.73^{A} (0.69–0.75)
Heterogeneous	77	60.2^{B} (36.2–62.9)	14.6^{B} (11.2–18.0)	0.75^{B} (0.68–0.77)
Distribution of vessels				
Benign				
Peripheral	18	32.7^{a} (26.3–41.3)	9.9^{a} (8.3–12.5)	0.70^{a} (0.68–0.74)
Internal	5	32.4^{a} (30.0–38.2)	9.4^{a} (9.3–11.0)	0.70^{a} (0.69–0.72)
Mixed	13	39.5^{b} (28.6–40.4)	11.3^{b} (9.2–12.1)	0.72^{a} (0.68–0.73)
Malignant				
Peripheral	30	42.2^{a} (36.2–48.3)	11.6^{a} (10.4–13.5)	0.72^{a} (0.68–0.74)
Internal	3	50.2^{ab} (48.4–52.1)	14.5^{ab} (14.1–14.6)	0.72^{b} (0.70–0.72)
Mixed	67	60.6^{b} (50.9–62.9)	14.7^{b} (13.2–18.0)	0.76^{b} (0.70–0.77)
Vascular pattern				
Benign				
Absent	18	32.7^{A} (26.3–41.3)	9.9^{A} (8.3–12.5)	0.70^{A} (0.68–0.74)
Spot	18	38.6^{A} (28.6–40.4)	11.0^{B} (9.2–12.0)	0.72^{A} (0.68–0.73)
Malignant				
Absent	30	42.2^{a} (36.2–48.3)	11.6^{a} (10.4–13.5)	0.72^{a} (0.68–0.74)
Spot	18	58.1^{b} (48.4–62.2)	14.6^{b} (13.2–16.5)	0.74^{b} (0.70–0.76)
Mesh	52	60.7^{b} (52.1–62.9)	14.7^{b} (14.1–18.0)	0.76^{b} (0.70–0.77)

^{A,B} Different letters indicate difference between the groups ($p < 0.01$, Mann–Whitney *U*–test).
^{a,b} Different letters indicate differences between the groups ($p < 0.01$, Kruskal–Wallis, Dunn's *post–hoc* multiple–comparison test).

Highlights

- The echotexture of neoplasm stroma is heterogeneous in a significant number of cases.
- The echographic texture influences the internal vessel dynamics.
- The distribution of vessels in a network pattern is predominant in the malignant neoplasm.
- Tumor vascularization morphology does not modify flow dynamics.
- Tumor pressure seems to be the main factor related to flow dynamics.

4 ARTIGO 3 - SERUM MEASUREMENT OF VASCULAR ENDOTHELIAL GROWTH FACTOR, INTERLEUKIN-8 AND ESTRADIOL, AND THE ULTRASOUND FINDINGS OF CANINE MAMMARY NEOPLASM

Artigo submetido no periódico:

BMC Cancer Journal

Serum measurement of vascular endothelial growth factor, interleukin-8 and estradiol, and the ultrasound findings of canine mammary neoplasm

Abstract

Background: The objective of this study was to evaluate the applicability of the association of serum markers related to vascularization with ultrasonographic findings as a complementary modality in classifying and characterization of canine breast cancers.

Methods: Fifty female dogs were evaluated and divided into two groups: a control group (healthy female dogs) and breast cancer group (female dogs with mammary carcinoma). The lesions were evaluated by ultrasonography (B-mode, color Doppler and spectral Doppler) and histopathological examination. Serum levels of vascular endothelial growth factor, interleukin (IL)-8, and estradiol were measured by immunoenzymatic assay in 37 female dogs with breast cancer and 13 healthy animals.

Results: Heterogeneous echotexture on ultrasonography showed an association with serum IL-8 levels. In addition, neoplasm vessel flow velocity and resistivity was positively correlated with serum vascular endothelial growth factor levels. Other ultrasonographic findings of breast cancers did not show significant correlations with serum markers.

Conclusions: The use of ultrasonography associated with serum markers may help in the characterization of breast cancers and favor the indication of an adjuvant therapy in patients with neoplasms with a greater likelihood of aggressiveness after surgical treatment.

Keywords: neoplasm vessels; serum marker; flow dynamics; echotexture; stroma; breast cancer.

Background

Neoplasm blood vessels are surprisingly heterogeneous and differ from their normal counterparts in organization, structure, and function. They develop either from venules and capillaries or from the remodeling of preexisting arteries and veins[1]. Angiogenesis is the initial mechanism in tumorigenesis and it is directly influenced by several factors[2-6]. Such factors are controlled not only by cancer cells but also by endothelial, inflammatory, and stromal cells[7-9].

Neoplasm vascularizíation is influenced by the biomechanics of blood flow and tissue metabolic demand[10,11,12], especially when there is a greater expression of vascular endothelial growth factor (VEGF) or associated chronic mechanical stress[11,12]. This process results in neoplasm vessels that are larger than their normal counterparts, with aberrant, vast, overbranched, and complex spatial distributions[1,3,13,14]; however, few vessels provide effective blood supply[1].

In breast cancer, the blood supply to the lesion increases, resulting in the development of anomalous vessels and a heterogeneous neoplasm stroma. These factors increase the dynamic stress of the flow in neoplasm vessels[15]. The main mechanical factors that interfere with vascular hemodynamics include shear stress, circumferential tension, blood cell concentration, the viscoelasticity of the adjacent tissue, and the constitution of the vascular wall[11,12,16,17]. Because of these conditions, breast cancers are more frequently affected by hemodynamic variations than benign lesions.[18-22]. In addition, increased shear stress and circumferential stress enhance exchange between blood flow and neoplasm cells[23]. This interaction may result in the increased levels of of relevant serum markers representing vascularization[7].

VEGF is a commonly investigated proangiogenic factor. However, there are few studies of the measurement of serum levels of this marker in veterinary oncology[24-26], and there are no reports relating these levels to the dynamics of neoplasm flow to our knowledge. Thus, the correlation of serum VEGF levels with the biological behavior of breast cancers would be a considerable benefit in the therapeutic and prognostic approach of female dogs with early-stage disease, because these levels are frequently evaluated in metastatic disease or progressive disease during treatment in humans[27].

The immune system reacts to the neoplasm[9,28,29]. As a consequence, cells release mediators that aid in interleukin (IL)-8 expression[29,30]. IL-8 is a proinflammatory and proangiogenic cytokine[31,32]. When derived from neoplasm cells, it can exert effects on growth, survival, invasion, angiogenesis,

metastasis, resistance, and neoplasm recurrence[33,34]. Higher IL-8 expression has already been associated with tissue hypoxia conditions[23,35]; therefore, correlation of IL-8 levels with vascular flow is hypothesized considering that IL-8 levels have been suggested as a prognostic marker[36,37].

The growth of lobular and alveolar tissue occurs primarily because of stimulation by sex hormones[38]. In humans, VEGF has been proposed to influence the development of breast tissue under steroid stimulation[39,40]. In addition, a positive correlation was observed between VEGF in neoplasm cells and the ERα/estradiol complex interaction[41]. Because serum estradiol may interfere in neoplasm VEGF expression, the most important proangiogenic factor, serum estradiol levels can be investigated when neoplasm vascularization is present.

The objective of this study was to associate ultrasonographic findings of breast cancers in dogs with serum markers related to vascularization such as VEGF, IL-8, and E2.

Methods

Characterization Of The Sample

A total of 102 unspayed female dogs were evaluated. Thirteen healthy dogs were selected for the control group (CG) and 37 dogs with breast cancers were selected for the breast cancer group (MCG). The evaluations were carried out in 2017 at the University of Passo Fundo Veterinary Hospital (HV-UPF). The classification between healthy and affected dogs was performed using an adapted version of an oncological staging protocol[42] for epithelial neoplasias. Thus, neoplasm size (T) was categorized into T1 (<3 cm), T2 (3–5 cm) and T3 (>5 cm); the involvement of regional lymph nodes (N) as either N0 (absent) or N1 (present); and distant metastasis (M) as either M0 (absent) or M1 (present). From this initial classification, stages 1 (T1, N0, and M0), 2 (T2, N0, and M0), 3 (T3, N0, and M0), 4 (any T, N1, and M0), and 5 (any T, any N, and M1) were characterized. The criteria for inclusion were absence of past history of oncological disease, presence of a single stage-1, stage-2, or stage-3, absence of inflammatory disease, estrus or cutaneous lesions, and one neoplasm with presence of vascular flow on color Doppler. Mammary glands and regional lymph nodes were surgically removed and submitted for histopathological examination. After excision, tissues were fixed in 10% formaldehyde and subsequently embedded in paraffin. Histological sections (5-μm thick) were obtained and stained with

hematoxylin and eosin. The classification of the neoplasm was performed using the method by Goldschmidt et al.[43], by the Laboratory of Animal Pathology at HV-UPF.

Ultrasonographic Study

After the clinical evaluation and before the surgical procedure, the mammary glands and the axillary and inguinal lymph nodes were examined with a 4–13-MHz linear transducer (Mylab 70; Esaote, Genoa, Italy). The dogs were examined in dorsal decubitus position and no chemical restraint was required. To decrease the subjectivity of the study, and because ultrasonography is operator-dependent, all examinations were performed by the same veterinarian. In the evaluation of breast cancers, the echotexture in B-mode and the vascularization through color Doppler were evaluated. On the basis of the identification of the flow, it was possible to observe the formation and distribution of the vessels. According to these characteristics, two patterns of vascular presentation in the stroma were proposed: (a) the mesh-like vascular pattern (MLVP), for numerous distorted tubular formations with excessive branching and a complex spatial distribution; (b) the spot-type vascular pattern (STVP), for branched tubular formations with a dispersed spatial distribution. In the evaluation of axillary and inguinal lymph nodes, the following exclusion criteria were used: a rounded shape, a narrow hilum, a hypoechogenic parenchyma, thin edges, the presence of posterior acoustic reinforcement, and peripheral or complex blood flow distribution; these findings are associated with lymphatic involvement[44]. The examination of neoplasm vessels began in B-mode, and images were obtained in the longitudinal and transverse planes. The ultrasound findings of the wall and the luminal content as well as the vessel's reaction to the transducer's mechanical pressure were evaluated whenever possible. Then color Doppler was used to evaluate the presence, direction, and characteristics of the flow. The spectral analysis was performed by pulsed Doppler, keeping the insonation angle (θ) $<60°$, and the sample volume was adjusted according to the vessel diameter. Pulse gain and pulse-repetition frequency were adjusted according to flow velocity. Peak systolic velocity (PSV), end diastolic velocity (EVD), and the resistive index ($RI = (PSV - EDV)/PSV$). The aforementioned analyses were performed three times each, using the mean of each value in this study. The images were digitally recorded and stored for analysis and subsequent calculations.

Serum Measurement of VEGF, Interleukin-8 and Estradiol

Three milliliters of blood was collected in a tube without anticoagulant. Samples were maintained at room temperature for up to 1 hour for clot retraction, and centrifuged at 2500 rpm for 5 minutes to promote serum separation. After pipetting, the serum was transferred to an Eppendorf plastic tube, identified, and frozen at −20°C. Serum VEGF measurement was performed using the Canine VEGF Quantikine® immunoenzymatic assay kit (R & D Systems®, Minneapolis, USA) using a specific monoclonal antibody for VEGF. Serine measurement of interleukin-8 (IL-8) was performed using the Canine CXCL8/IL-8 Quantikine® immunoenzymatic assay kit (R & D Systems®, Minneapolis, USA) using a specific monoclonal antibody for canine IL-8. Serum estradiol (E2) levels were measured by the Parameter™ estradiol kit (R & D Systems®, Minneapolis, USA) using a specific monoclonal antibody for estradiol. Manufacturer's guidelines for each of the kits were followed for the evaluations. Optical densities were measured at 450 nm in an immunoenzymatic assay reader (Asys UVM 340). The intensities of the reactions were proportional to the levels of VEGF, IL-8, and estradiol. Optical densities were calculated on the basis of the adjustment curves using Plate Digiread® software.

Statistical Analysis

The variables were tested for their normality using the Kolmogorov–Smirnov test. However, none the variables obtained (VEGF, IL-8, and E2) in either of the categories linked to the groups (control and breast carcinoma) or intratumoral characteristics (neoplasm size, histological grade, echotexture and vessel distribution) presented normal distribution. Thus, they were analyzed by either the Mann–Whitney U-test or the Kruskal–Wallis test, followed by Dunn's multiple-comparison *post hoc* test. In addition, a Spearman correlation was performed to verify possible relationships between hemodynamics (peak systolic velocity, end diastolic velocity, and resistivity) and serum markers (VEGF, IL-8 and E2). Data were considered significantly different when probability was <5% ($p < 0.05$). Graphpad Prism®, version 6.0 was used for the analysis.

The study protocol followed the appropriate guidelines and was approved by the Ethics Committee on Animal Use of the UPF, Passo Fundo, State of Rio Grande do Sul, Brazil, registered with the number 030/2017.

Results

Sample Description

Neoplasm stromal echotexture, vascular presentation pattern, flow velocity, RI, histological grade of breast cancer, and serum levels of VEGF, IL-8, and E2 from 50 unspayed canine females aged 3–15 years were evaluated. CG was composed of 13 healthy dogs, and MCG had 37 females diagnosed with breast cancer. MC diagnoses consisted of 12 simple type, nine complex type, six solid, five adenosquamous, and five mixed type tumors. Twenty-seven neoplasms were grade I, six grade II, only one grade III; three neoplasms were not graded. At ultrasonographic examination, MCG obtained five cases of homogeneous echotexture of the stroma, but heterogeneous echotexture of the stroma was seen in in 32 cases of mammary carcinoma (MC). In addition, vascular flow was identified in the neoplasm stroma in almost 100% of the cases. MLVP vascularization pattern was observed in 25 cases, whereas STVP vascularization pattern was observed in 11. One cases showed an absence of any vascular pattern (Table 1); in this case, the flow presented had exclusively peripheral distribution.

VEGF Serum Measurement

No statistically significant difference ($p > 0.05$) in serum VEGF levels was observed between CG and MCG (Figure 1). Similarly, no significant difference was found when MCs were categorized by histological grade, stromal echotexture, and vascular distribution pattern (Table 1). However, there was a positive ($p < 0.01$) and moderate correlation (Figure 2) between serum VEGF levels and PSV ($r = 0.50$), EDV ($r = 0.41$), and RI ($r = 0.46$).

Interleukin-8 Serum Measurement

A difference in IL-8 levels ($p < 0.01$) was observed between CG and MCG (Figure 1), and the difference between CG and grade-I, grade-II, and nongraded neoplasms was also significant when the

CG and MCG were compared with regard to heterogeneous echotexture, MLVP, STVP (Table 1). However, the same significance was not observed between grade-I, grade-II, and nongraded neoplasms, as well as between CG and homogeneous echotexture, STVP, and MLVP ($p > 0.05$). In addition, there was no correlation ($p < 0.01$) between serum IL-8 levels and flow velocities, similar to the relationship between serum IL-8 levels and resistivity (Figure 3).

Estradiol Serum Measurement

Serum estradiol levels were not different ($p > 0.05$) between CG and MCG (Figure 1). Serum estradiol levels were not significantly different either among the other parameters observed: histological grade, stromal echotexture, and vascular presentation pattern (Table 1). Likewise, there was no correlation ($p > 0.05$) between serum estradiol level, the flow velocities (PSV and EDV), and RI (Figure 4).

Discussion

Mammary neoplasms (MNs) are the most common neoplastic disease in unspayed elderly female dogs, and most MNs are malignant. Among breast cancers, mammary carcinomas (MCs) are the most prevalent in domestic canines[38,45-47], as we found in the present study. Canine MC (CMC) may be associated with more than one lesion in the mammary chain, with different lengths, times of evolution, histological diagnoses, and grades; however, CMC may or may not present local and distant metastasis[47]. Mastectomy is associated with cure in about half of breast cancer cases, whereas the other half is related to recurrence or the development of metastatic foci[47,48]. Based on this information, only CMC stages I, II, and III[42] were studied, considering the need to evaluate cases with some probability of cure with the use of adjuvant therapies[36,38].

The characteristics of neoplasm vascularization are correlated with malignancy[8,19], because tissue blood circulation is crucial for the growth and formation of metastatic foci[5,16,49,50]. The biomechanics of vascular flow, along with the demand for breast cancer perfusion, are important and constant influences on this vascularization process[10,11,12]. This is because these factors promote an increase in new vessels, particularly in malignant cases[19]. However, these vessels are generally

ineffective[1] in providing the needs of cancer cells, because of which they are associated with areas of metabolic insufficiency, hypoxia, ischemia, and necrosis[6,35,51]. This results in connective tissue reactions in the neoplasm stroma, with increased levels of collagen, fibrosis, cell density, fluids, plasma proteins, blood cells in the interstitium, and adjacent tissue involvement[15,52]. This manifests in the form of the high number of CMCs with heterogeneous echotexture in our ultrasonographic evaluation.

The increased serum IL-8, identified in breast cancers with heterogeneous echotexture when compared to those with homogeneous echotexture and to healthy female dogs, probably was a result of stromal reactions[15,52]. This is considering the greater expression had already been reported in cancer cells[31,32,53], in the neoplasm microenvironment[33,54,55], in inflammation[29,34,56], in hypoxia[23,28,35], in the involvement of lymph nodes, and in the presence of metastases[36,37,57]. However, the data on the quantification of IL-8 levels in the serum of female dogs with breast cancer is scarce, and the few existing studies have shown higher IL-8 serum levels when compared to healthy patients[36,37]. In women, the same increase was not observed in the initial stages without lymph node involvement and the presence of metastases[30,57,58]. Our data may be related to the large number of heterogeneous MNs, because when stromal echotexture was tested, serum IL-8 levels in breast cancers were higher in stages I, II, and III. Thus, our findings may suggest the need for further investigation of CMCs with heterogeneous echotexture, as they showed an increase in serum IL-8 levels, which was also seen in cases with lymph node involvement and the presence of metastasis in humans[30,57,58].

The positive association between IL-8 levels and heterogeneous echotexture may indicate greater neoplasm stromal stiffness[15,52], which was not sufficient to change the dynamics of the vessels. This is because it was not possible to observe a correlation between flow velocity (Vfl) and RI and IL-8 serum levels. The histological grade, which is similarly associated with greater tissue stiffness[52] and cellular activity[45,47,59], did not alter IL-8 levels in breast cancer.

Angiogenesis is the primary mechanism for neoplasm vascularization and an indicator of malignancy[4,47,60], although breast cancers also obtain their vascular supply through other mechanisms, such as vasculogenic mimicry, angioblast recruitment, and vascular cooptation[10]. Angiogenesis is induced surprisingly early during the development of cancer and can be controlled by cancer cells, endothelial cells, the neoplasm microenvironment[6-9], and inflammatory cells[29,61]. Hypoxia, metabolic

stimuli[6,8,24,35], and biomechanical factors constantly boost this formation of new vessels and regulate the neoplasm blood flow[4,12,53]. The hypervascularization and flow increase associated with breast cancers[19,20,22] increase the interaction between hemodynamics and cancer cells, and consequently strengthen the metastatic phenotype[5,63,64]. These events favor an increase of proangiogenic molecules, such as VEGF, secreted by cancer cells[1] in situations of mechanical stress[11,12], which is in line with our observations of a positive correlation between serum vascular pattern-independent VEGF levels, Vfl, and RI.

VEGF is the main proangiogenic factor[7,13,65]; it is produced by cancer, endothelial, and stromal cells[39,63], and it is related to several stages of neoplasm vascularization. This is because it enables an increase in vascular permeability, stimulates the migration and proliferation of endothelial cells, helps in the maturation of new blood vessel precursors, and promotes vasoactive and chemotactic molecules[8,66,67]. In addition, increased serum VEGF, especially in MNs, is correlated with increased aggressiveness[26,67,68]. Thus, Vfl and RI changes associated with increased VEGF may suggest the need for adjuvant therapy in oncological stages I, II, and III in canines.

Formed and remodeled neoplasm vessels have a heterogeneous conformation, in the same way as the breast cancer stroma. Vascularization development and adaptation results in numerous aberrant, distorted, and dilated vessels with poor endothelial lining, excessive branching, collapsed areas, complex spatial distribution, and anomalous/permeable junctions[1,3,14,21]. These morphological vascular variations may also alter the flow dynamics in the neoplasm and enable a greater stimulation of cancer and endothelial cells[5,6,63] and the neoplasm microenvironment[7,14,23,62,69]. In spite of this, our findings showed higher IL-8 serum levels in breast cancers only when compared to healthy female dogs, without showing an increase in the MLVP when compared to the STVP. This indicates that the characterization of color Doppler vascularity presentation may not have been effective in assessing flow complexity and correlation with VEGF and IL-8. Therefore, it may be necessary to perform contrast-enhanced ultrasonographic techniques to improve the accuracy of vascular pattern evaluation[15,21,22].

The heterogeneity of breast cancers, resulting from the proliferation of cancer cells, tissue support, and vascularization, can compress vessels, impair tissue perfusion, and regulate the expression of factors related to tissue hypoxia[13]. However, no such relationship was found with serum VEGF levels.

Another factor associated with increased serum VEGF in breast cancers is the histological grade, which may be correlated with a higher grading [27,67,68] and to a greater stiffness of the neoplasm stroma[52], suggesting a relationship between neovascularization and biological behavior[38]. However, such a comparison was not possible because of the occurrence of only one case of MC degree III, whereas no significant differences were observed in both graded and nongraded neoplasms.

In mammals, steroid hormones play an important role in the development of the alveolar lobe of the mammary gland and are associated with CMC pathogenesis[38]. In humans, the influence of sex steroids on VEGF expression, when associated with tissue growth and vascular supply, has been proposed[39,40]; this is because there is a positive regulation of VEGF in cancer cells by the interaction between E2 and its receptor[39,40,41]. Thus, the production of neoplasm VEGF may be influenced by ovarian activity[39,40,41]. In our findings, there was no difference in serum E2 levels between the groups; this suggests the absence of estrogenic interference in VEGF serum levels, even when MCs are categorized according to histological grade, stromal echotexture, and vascular presentation pattern[39,65,66]. A possible lack of development of neoplasm mammary tissue by steroid stimulus[38] was also suggested by the absence of a difference in flow dynamics between the serology of healthy female dogs in contrast to those with breast cancers.

Conclusion

In canine breast cancers, the measurement of VEGF, IL-8, and E2 and the characterization of stroma and vascularization were attractive for the attribute study of stages I, II, and III, and for the possibility of helping in the indication of adjuvant therapy in MC. The dynamics of blood flow directly influenced VEGF expression, the main neoplasm angiogenesis marker, demonstrating the importance of correlating serum VEGF levels, Doppler flow rates, and resistivity in the characterization of breast cancer. This is importan considering that this association could help in identifing patients with greater potential to develop metastatic foci. IL-8 levels increased when the stroma presented heterogeneous echotexture, which brought these breast cancers without local or distant the presence of metastases closer to more aggressive characteristics of the disease. This finding suggests the use of this association of findings for identifying patients with greater potential for neoplasm aggressiveness. Our findings on

E2 measurement raised a suspicion about its influence on serum VEGF levels in patients with MC, and these two factors should be investigated together.

References

1. Nagy JA, Chang SH, Shih SC, Dvorak AM, Dvorak HF. Heterogeneity of the tumor vasculature. Semin Thromb Hemost. 2010;36:321-331. https://doi.org/10.1055/s-0030-1253454.
2. Hanahan D, Folkman J. Patterns and emerging mechanisms of the angiogenic switch during tumorigenesis. Cell. 1996;86:353-364. https://doi.org/10.1016/S0092-8674(00)80108-7.
3. Pathak AP, Penet M-F, Bhujwalla ZM. MR molecular imaging of tumor vasculature and vascular targets. Adv Genet. 2010;69:1-30. https://doi:10.1016/S0065-2660(10)69010-4.
4. Sleeckx N, Van Brantegem L, Van den Eynden G, Fransen E, Casteleyn C, Van Cruchten S, et al. Angiogenesis in canine mammary tumours: A morphometric and prognostic study. J Comp Pathol. 2014;150:175-183. https://doi.org/10.1016/j.jcpa.2013.09.006.
5. Viger L, Denis F, Rosalie M, Letellier C. A cancer model for the angiogenic switch. J Theor Biol. 2014;360:21-33. https://doi.org/10.1016/j.jtbi.2014.06.020.
6. Li S, Meng W, Guan Z, Guo Y, Han X. The hypoxia-related signaling pathways of vasculogenic mimicry in tumor treatment. Biomed Pharmacother. 2016;80:127-135. https://doi.org/10.1016/j.biopha.2016.03.010.
7. Hanahan D, Weinberg RA. Hallmarks of cancer: the next generation. Cell. 2011;144:646-674. https://doi.org/10.1016/j.cell.2011.02.013.
8. Saponaro C, Malfettone A, Ranieri G, Danza K, Simone G, Paradiso A, et al. VEGF, HIF-1α expression and MVD as an Angiogenic Network in Familial Breast Cancer. PLOS ONE. 2013;8:e53070. https://doi.org/10.1371/journal.pone.0053070.
9. Santos AA, Matos AJF. Advances in the understanding of the clinically relevant genetic pathways and molecular aspects of canine mammary tumours. Part 2: Invasion, angiogenesis, metastasis and therapy. Vet J. 2015;205:144-153. https://doi.org/10.1016/j.tvjl.2015.03.029.
10. Auguste P, Lemiere S, Larrieu-Lahargue F, Bikfalvi A. Molecular mechanisms of tumor vascularization. Crit Rev Oncol Hematol. 2005;54:53-61. https://doi.org/10.1016/j.critrevonc.2004.11.006.

11. Lee GS, Filipovic N, Miele LF, Lin M, Simpson DC, Giney B, et al. Blood flow shapes intravascular pillar geometry in the chick chorioallantoic membrane. J Angiogenes Res. 2010;2:1-9. https://doi.org/10.1186/2040-2384-2-11.
12. Clegg LE, Mac Gabhann F. Systems biology of the microvasculature. Integr Biol. 2015;7:498-512. https://doi.org/10.1039/C4IB00296B.
13. Carmeliet P, Jain RK. Molecular mechanisms and clinical applications of angiogenesis. Nature. 2011;473:298-307. https://doi.org/10.1038/nature10144.
14. Kim E, Stamatelos S, Cebulla J, Bhujwalla ZM, Popel AS, Pathak AP. Multiscale imaging and computational modeling of blood flow in the tumor vasculature. Ann Biomed Eng. 2012;40:2425-2441. https://doi.org/10.1007/s10439-012-0585-5.
15. Feliciano MAR, Uscategui RAR, Maronezi MC, Simões APR, Silva P, Gasser B, et al. Ultrasonography methods for predicting malignancy in canine mammary tumors. PLOS ONE. 2017;12:e0178143. https://doi.org/10.1371/journal.pone.0178143.
16. Carmeliet P. Mechanisms of angiogenesis and arteriogenesis. Nat Med. 2000;6:389-395. https://doi.org/10.1038/74651.
17. Gompper G, Fedosov DA. Modeling microcirculatory blood flow: current state and future perspectives. Wiley Interdiscip Rev Syst Biol Med. 2016;8:157-168. https://doi.org/10.1002/wsbm.1326.
18. Feliciano MAR, Vicente WRR, Silva MAM. Conventional and Doppler ultrasound for the differentiation of benign and malignant canine mammary tumours. J Small Anim Pract. 2012;53:332-337. https://doi.org/10.1111/j.1748-5827.2012.01227.x.
19. Huang YH, Chen JH, Chang YC, Huang CS, Moon WK, Kuo WJ, et al. Diagnosis of solid breast tumors using vessel analysis in three-dimensional power Doppler ultrasound images. J Digit Imaging. 2013;26:731-739. https://doi.org/10.1007/s10278-012-9556-5.
20. Davoudi Y, Borhani B, Rad MP, Matin N. The role of Doppler sonography in distinguishing malignant from benign breast lesions. J Med Ultrasound. 2014;22:92-95. https://doi.org/10.1016/j.jmu.2013.12.001.

21. Stanzani D, Chala LF, Barros Nd, Cerri GG, Chammas MC. Can Doppler or contrast-enhanced ultrasound analysis add diagnostically important information about the nature of breast lesions? Clinics. 2014;69:87-92. https://doi.org/10.6061/clinics/2014(02)03.
22. Yongfeng Z, Ping Z, Wengang L, Yang S, Shuangming T. Application of a novel microvascular imaging technique in breast lesion evaluation. Ultrasound Med Biol. 2016;42:2097-2105. https://doi.org/10.1016/j.ultrasmedbio.2016.05.010.
23. Silvestre JS, Smadja DM, Lévy BI. Postischemic revascularization: from cellular and molecular mechanisms to clinical applications. Physiol Rev. 2013;93:1743-1802. https://doi.org/10.1152/physrev.00006.2013.
24. Moschetta MG, Gelaleti GB, Maschio LB, Jardim BV, Leonel C, Ferreira LC, et al. Serum and molecular assessment of vascular endothelial growth factor (VEGF) and hypoxia-inducible factor 1α (HIF-1α) in canine mammary tumors. BMC Proc. 2013;7:49. https://doi.org/10.1186/1753-6561-7-S2-P49.
25. Moschetta MG, Maschio LB, Jardim-Perassi BV, Gelaleti GB, Lopes JR, Leonel C, et al. Prognostic value of vascular endothelial growth factor and hypoxia-inducible factor 1α in canine malignant mammary tumors. Oncol Rep. 2015;33:2345-2353. https://doi.org/10.3892/or.2015.3856.
26. Kato Y, Asano K, Mogi T, Kutara K, Teshima K, Edamura K, et al. Clinical significance of circulating vascular endothelial growth factor in dogs with mammary gland tumors. J Vet Med Sci. 2007;69:77-80. https://doi.org/10.1292/jvms.69.77
27. Ali EM, Sheta M, El Mohsen MA. Elevated serum and tissue VEGF associated with poor outcome in breast cancer patients. Alexandria J Med. 2011;47:217-224. https://doi:10.1016/j.ajme.2011.07.003.
28. Angelo LS, Kurzrock R. Vascular endothelial growth factor and its relationship to inflammatory mediators. Clin Cancer Res. 2007;13:2825-2830. https://doi.org/10.1158/1078-0432.CCR-06-2416.

29. Dirkx AEM, oude Egbrink MGA, Wagstaff J, Griffioen AW. Monocyte/macrophage infiltration in tumors: modulators of angiogenesis. J Leukoc Biol. 2006;80:1183-1196. https://doi.org/10.1189/jlb.0905495.
30. Derin D, Soydinc HO, Guney N, Tas F, Camlica H, Duranyildiz D, et al. Serum IL-8 and IL-12 levels in breast cancer. Med Oncol. 2007;24:163-168. https://doi.org/10.1007/BF02698035.
31. Waugh DJJ, Wilson C. The interleukin-8 pathway in cancer. Clin Cancer Res. 2008;14:6735-6741. https://doi.org/10.1158/1078-0432.CCR-07-4843.
32. Zuccari DA, Castro R, Gelaleti GB, Mancini UM. Interleukin-8 expression associated with canine mammary tumors. Genet Mol Res. 2011;10:1522-1532. https://doi.org/10.4238/vol10-3gmr1145.
33. Lee YS, Choi I, Ning Y, Kim NY, Khatchadourian V, Yang D, et al. Interleukin-8 and its receptor CXCR2 in the tumour microenvironment promote colon cancer growth, progression and metastasis. Br J Cancer. 2012;106:1833-1841. https://doi.org/10.1038/bjc.2012.177.
34. Mohamed MM, Al-Raawi D, Sabet SF, El-Shinawi M. Inflammatory breast cancer: new factors contribute to disease etiology: a review. J Adv Res. 2014;5:525-536. https://doi.org/10.1016/j.jare.2013.06.004.
35. Gilkes DM, Semenza GL. Role of hypoxia-inducible factors in breast cancer metastasis. Future Oncology. 2013;9:1623-1636. https://doi.org/10.2217/fon.13.92.
36. Gelaleti GB, Jardim BV, Leonel C, Moschetta MG, Zuccari DAP. Interleukin-8 as a prognostic serum marker in canine mammary gland neoplasias. Vet Immunol Immunopathol. 2012;146:106-112. https://doi.org/10.1016/j.vetimm.2012.02.005.
37. de Andrés PJ, Illera JC, Cáceres S, Díez L, Pérez-Alenza MD, Peña L. Increased levels of interleukins 8 and 10 as findings of canine inflammatory mammary cancer. Vet Immunol Immunopathol. 2013;152:245-251. https://doi.org/10.1016/j.vetimm.2012.12.010.
38. Queiroga FL, Raposo T, Carvalho MI, Prada J, Pires I. Canine mammary tumours as a model to study human breast cancer: most recent findings. In Vivo. 2011;25:455-465. https://www.researchgate.net/publication/51130760

39. Santos AA, Oliveira JT, Lopes CC, Amorim IF, Vicente CM, Gärtner FR, et al. Immunohistochemical expression of vascular endothelial growth factor in canine mammary tumours. J Comp Pathol. 2010;143:268-275. https://doi.org/10.1016/j.jcpa.2010.04.006.

40. Hoffmann B, Schuler G. Receptor blockers - General aspects with respect to their use in domestic animal reproduction. Anim Reprod Sci. 2000;60–61:295–312. https://doi.org/10.1016/S0378-4320(00)00129-9

41. Fan F, Schimming A, Jaeger D, Podar K. Targeting the Tumor Microenvironment: Focus on Angiogenesis. *Journal of Oncology*. 2012;2012:281261. https://doi:10.1155/2012/281261.

42. Rutteman G, Withrow S, Macewen E. Tumors of the mammary gland. In: Withrow S, Macewen E, Small Animal Clinical Oncology. 3. Educativa. Phila: W B Saunders; 2001:726-756.

43. Goldschmidt MH, Peña L, Rasotto R, Zappulli V. Classification and grading of canine mammary tumors. Vet Pathol. 2011;48:117-131. https://doi.org/10.1177/0300985810393258.

44. Carvalho FC. Ultrassonografia Doppler de linfonodos [Doppler ultrasonography of lymph nodes]. In: Carvalho FC. Ultrassonografia Doppler em pequenos animais [Doppler ultrasonography of small animals]. Editora Roca, São Paulo, Brazil; 2009:178-183.

45. Sleeckx N, de Rooster H, Veldhuis Kroeze EJ, Van Ginneken C, Van Brantegem L. Canine mammary tumours, an overview. Reprod Domest Anim. 2011;46:1112-1131. https://doi.org/10.1111/j.1439-0531.2011.01816.x.

46. Sorenmo KU, Rasotto R, Zappulli V, Goldschmidt MH. Development, anatomy, histology, lymphatic drainage, clinical features, and cell differentiation markers of canine mammary gland neoplasms. Vet Pathol. 2011;48:85-97. https://doi.org/10.1177/0300985810389480.

47. Diessler ME, Castellano MC, Portiansky EL, Burns S, Idiart JR. Canine mammary carcinomas: influence of histological grade, vascular invasion, proliferation, microvessel density and VEGFR2 expression on lymph node status and survival time. Vet Comp Oncol. 2017;15:450-461. https://doi.org/10.1111/vco.12189.

48. Clemente M, Pérez-Alenza MD, Peña L. Metastasis of canine inflammatory versus non-inflammatory mammary tumours. J Comp Pathol. 2010;143:157-163. https://doi.org/10.1016/j.jcpa.2010.02.002.

49. Folkman J. Role of angiogenesis in tumor growth and metastasis. Semin Oncol. 2002;29, asonc02906q0015. https://doi.org/10.1053/sonc.2002.37263:15-18.

50. Kerbel RS. Tumor Angiogenesis. *The New England journal of medicine*. 2008;358(19):2039-2049. https://doi:10.1056/NEJMra0706596.

51. Vaupel P, Mayer A. Hypoxia in cancer: significance and impact on clinical outcome. Cancer Metastasis Rev. 2007;26:225-239. https://doi.org/10.1007/s10555-007-9055-1.

52. Zhou J, Zhan W, Chang C, Zhang J, Yang Z, Dong Y, et al. Role of acoustic shear wave velocity measurement in characterization of breast lesions. J Ultrasound Med. 2013;32:285-294. https://doi.org/10.7863/jum.2013.32.2.285

53. Lin Y, Huang R, Chen L, Li S, Shi Q, Jordan C, et al. Identification of interleukin-8 as estrogen receptor-regulated factor involved in breast cancer invasion and angiogenesis by protein arrays. Int J Cancer. 2004;109:507-515. https://doi.org/10.1002/ijc.11724.

54. Yuan A, Chen JJW, Yao PL, Yang PC. The role of interleukin-8 in cancer cells and microenvironment interaction. Front Biosci. 2005;10:853-865. https://doi.org/10.1093/geront/gns022.

55. Raposo TP, Pires I, Carvalho MI, Prada J, Argyle DJ, Queiroga FL. Tumour-associated macrophages are associated with vascular endothelial growth factor expression in canine mammary tumours. Vet Comp Oncol. 2015;13:464-474. https://doi.org/10.1111/vco.12067.

56. Shahzad A, Knapp M, Lang I, Köhler G. Interleukin 8 (IL-8) - a universal biomarker? Int Arch Med. 2010;3:11. https://doi.org/10.1186/1755-7682-3-11.

57. Ma Y, Ren Y, Dai ZJ, Wu CJ, Ji YH, Xu J. IL-6, IL-8 and TNF-α levels correlate with disease stage in breast cancer patients. Adv Clin Exp Med. 2017;26:421-426. https://doi.org/10.17219/acem/62120.

58. Benoy IH, Salgado R, Van Dam P, Geboers K, Van Marck E, Scharpé S, et al. Increased serum interleukin-8 in patients with early and metastatic breast cancer correlates with early dissemination and survival. Clin Cancer Res. 2004;10:7157-7162. https://doi.org/10.1158/1078-0432.CCR-04-0812.

59. Estrela-Lima A, Araújo MSS, Soares RP, Ribeiro LGR, Damasceno KA, Costa AT, et al. Plasma biomarkers profile of female dogs with mammary carcinoma and its association with clinical and pathological features. Vet Comp Oncol. 2016;14:88-100. https://doi.org/10.1111/vco.12070.

60. Folkman J. Angiogenesis in cancer, vascular, rheumatoid and other disease. Nat Med. 1995;1:27-30. https://doi.org/10.1038/nm0195-27.

61. Clemente M, Sánchez-Archidona AR, Sardón D, Díez L, Martín-Ruiz A, Caceres S, et al. Different role of COX-2 and angiogenesis in canine inflammatory and non-inflammatory mammary cancer. Vet J. 2013;197:427-432. https://doi.org/10.1016/j.tvjl.2013.02.009.

62. Logsdon EA, Finley SD, Popel AS, Mac Gabhann F. A systems biology view of blood vessel growth and remodelling. J Cell Mol Med. 2014;18:1491-1508. https://doi.org/10.1111/jcmm.12164.

63. Holopainen T, Bry M, Alitalo K, Saaristo A. Perspectives on lymphangiogenesis and angiogenesis in cancer. J Surg Oncol. 2011;103:484-488. https://doi.org/10.1002/jso.21808.

64. Mori N, Mugikura S, Takahashi S, Ito K, Takasawa C, Li L, et al. Quantitative analysis of contrast-enhanced ultrasound imaging in invasive breast cancer: A novel technique to obtain histopathologic information of microvessel density. Ultrasound Med Biol. 2017;43:607-614. https://doi.org/10.1016/j.ultrasmedbio.2016.11.009.

65. Millanta F, Caneschi V, Ressel L, Citi S, Poli A. Expression of vascular endothelial growth factor in canine inflammatory and non-inflammatory mammary carcinoma. J Comp Pathol. 2010;142:36-42. https://doi.org/10.1016/j.jcpa.2009.06.004.

66. Qiu CW, Lin DG, Wang JQ, Li CY, Deng GZ. Expression and significance of PTEN and VEGF in canine mammary gland tumours. Vet Res Commun. 2008;32:463-472. https://doi.org/10.1007/s11259-008-9049-7.

67. Shivakumar S, Prabhakar BT, Jayashree K, Rajan MGR, Salimath BP. Evaluation of serum vascular endothelial growth factor (VEGF) and microvessel density (MVD) as prognostic indicators in carcinoma breast. J Cancer Res Clin Oncol. 2009;135:627-636. https://doi.org/10.1007/s00432-008-0497-9.

68. Duranyildiz D, Camlica H, Soydinc HO, Derin D, Yasasever V. Serum levels of angiogenic factors in early breast cancer remain close to normal. Breast. 2009;18:26-29. https://doi.org/10.1016/j.breast.2008.09.004.

69. Kareva I. Escape from tumor dormancy and time to angiogenic switch as mitigated by tumor-induced stimulation of stroma. J Theor Biol. 2016;395:11-22. https://doi.org/10.1016/j.jtbi.2016.01.024.

Table 1. Characterization of mammary neoplasms in female dogs by ultrasonographic examination, according to the histopathological diagnosis of breast cancers.

	Number of neoplasms	VEGF (pg/mL)	IL-8 (pg/mL)	Estradiol (pg/mL)
Histological grade				
Control	13	35.1[a] (10.1–51.8)	1013.4[a] (951.3–1029.7)	71.8[a] (9.20–102.80)
Grade 1	27	37.0[a] (6.4–98.2)	1029.7[b] (909.7–1041.4)	82.6[a] (9.10–166.00)
Grade 2	6	43.0[a] (33.3–54.6)	1032.7[b] (1018.5–1053.5)	60.5[a] (1.80–140.00)
Grade 3	1	26.8 (---)	1047.0 (---)	111.8 (---)
Nongraded	3	37.0[a] (26.8–136.6)	1041.4[b] (1035.3–1047.0)	68.0[a] (52.20–80.80)
Echotexture				
Control	13	35.1[a] (10.1–51.8)	1013.4[a] (951.3–1029.7)	71.8[a] (9.20–102.80)
Homogeneous	5	69.5[a] (15.7–98.2)	1035.3[a] (909.7–1041.4)	72.3[a] (35.30–99.20)
Heterogeneous	32	37.0[a] (6.4–136.3)	1035.3[b] (1003.1–1053.5)	81.7[a] (1.77–166.00)
Vascular pattern				
Control	13	35.1[a] (10.1–51.8)	1013.4[a] (951.3–1029.7)	71.8[a] (9.20–102.80)
Absent	1	15.7 (---)	1029.7 (---)	99.2 (---)
Spot	11	37.0[a] (28.6–98.2)	1035.3[b] (909.7–1053.3)	63.0[a] (15.60–125.80)
Mesh	25	37.9[a] (6.4–136.3)	1035.3[b] (1003.1–1053.5)	84.0[a] (1.77–166.00)

[a,b]Different letters indicate differences between groups ($p < 0.01$, Kruskal–Wallis, Dunn's multiple-comparison test).

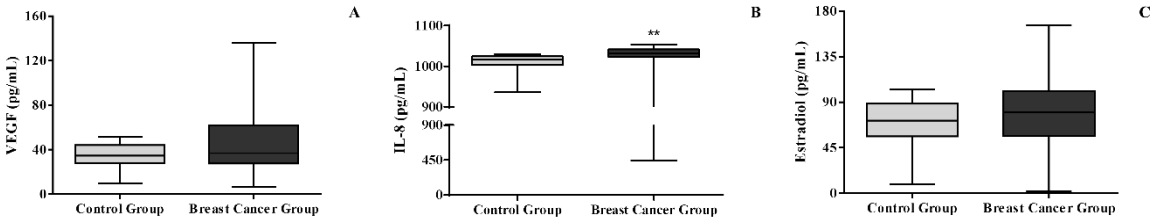

Figure 1. Serological measurement of the control and breast cancer groups. Serum vascular endothelial growth factor levels (A). Serum interleukin-8 levels (B). Serum estradiol levels (C). ** Indicates difference between groups ($p < 0.01$, Mann–Whitney U-Test)

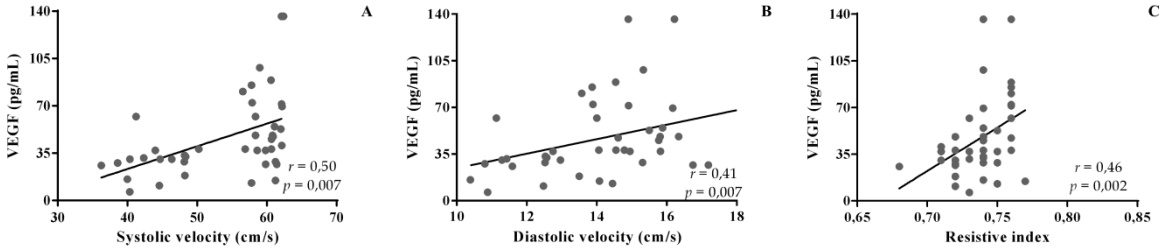

Figure 2. Positive correlations between serum levels of vascular endothelial growth factor and peak systolic velocity (A), end diastolic velocity (B), and resistive index (C) (r – Spearman's correlation coefficient)

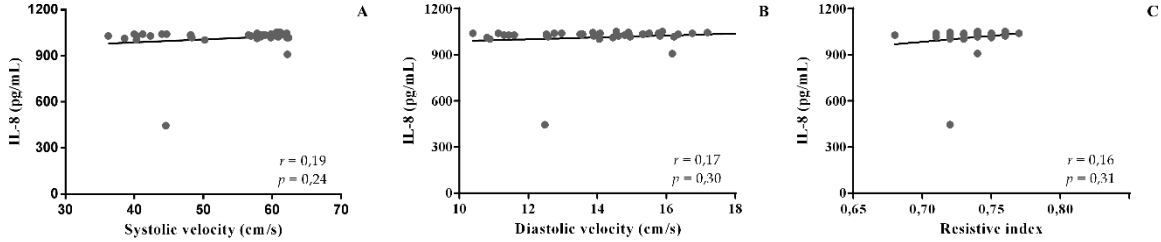

Figure 3. Absence of correlation between serum interleukin-8 levels and peak systolic velocity (A), end diastolic velocity (B), and resistive index (C). (r – Spearman's correlation coefficient)

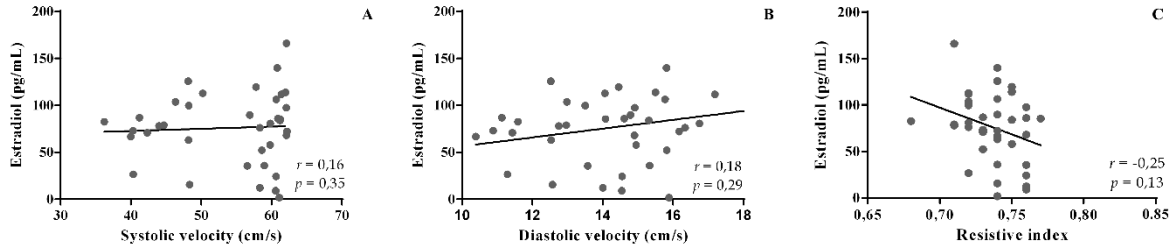

Figure 4. Correlation between serum estradiol levels and peak systolic velocity (A), end diastolic velocity (B), and resistivity index (C) (r – Spearman's correlation coefficient)

5 DISCUSSÃO

O estudo ecográfico do neoplasma mamário maligno demonstrou ser um método conciso na detecção da vascularização, como já evidenciado em outros estudos (KWAK et al., 2008; FELICIANO et al., 2012; CANDELARIA et al., 2013; DAVOUDI et al., 2014). O neoplasma maligno apresentou ao Doppler colorido uma grande quantidade de vasos detectáveis, com fluxo laminar (SOLER et al., 2016) e sugeriu relação entre os atributos vasculares ao Doppler e o comportamento biológico neoplásico.

A distribuição ampla dos vasos nos neoplasmas malignos, modificaram as Vfl, com maior intensidade quando distribuídos ao mesmo tempo no interior e na periferia da lesão, estando estes resultados possivelmente associados a maior necessidade de fluxo (SOLER et al., 2016). O IR foi maior nos vasos internos, sendo justificado pelo efeito mecânico extra vascular, já que o neoplasma maligno geralmente é mais rígido e menos viscoelástico (ZHOU et al., 2013; FELICIANO et al., 2017).

Na neoplasia mamaria canina, o tamanho do neoplasma pode sugerir a diferenciação entre benignos e maligno (FERREIRA et al., 2009). Do mesmo modo, que existe uma associação positiva entre a agressividade do neoplasma maligno e a intensidade de fluxo (LEE et al., 1996; HUANG et al., 2013; SOLER et al., 2016). Assim, atributos associados a vascularização deveriam ser empregados no estádio clínico oncológico do neoplasma mamário canino, visto que, a formação vascular pode ocorrer antes da progressão do tamanho tumoral (STANZANI et al., 2014), através de mecanismos que transformam pequenas lesões avasculares para um fenótipo vascular (AUGUSTE et al., 2005), exceto quando no estado de dormência, que alguns neoplasmas malignos manifestam, apoiados na falta de estímulos ou na presença de inibidores vasculares (KAREVA, 2016).

As Vfl e o IR acompanharam o tamanho tumoral e foram incrementados nos neoplasmas maiores, possivelmente em decorrência da maior demanda metabólica (ZHAO et al., 2004; AUGUSTE et al., 2005; KIM et al., 2012; LOGSDON et al., 2014; KAREVA, 2016), que se torna mais rígido e menos viscoelástico (ZHOU et al., 2013; FELICIANO et al., 2017). O grau histológico também já foi correlacionado a maior rigidez do neoplasma mamário (ZHOU et al., 2013), entretanto, o grau I, II e não graduados não demonstraram influência na hemodinâmica vascular dos neoplasmas, nos estádios iniciais. Desta maneira a maior rigidez pode estar associada ao grau III, que devido a baixa incidência não pode ser analisado.

Outra característica, que pode ser interpretada em conjunto com a vascularização, nos estádios I, II e III foi a ecotextura do neoplasma (CLEMENTE et al., 2010; DIESSLER et al.,

2017). Considera-se que a heterogenicidade tecidual dos neoplasmas malignos esteja relacionada as variações hemodinâmicas ocasionadas pela alteração de perfusão e dano tecidual no ambiente do neoplasma (ZHOU et al., 2013; LOGSDON et al., 2014; STAMATELOS et al., 2014; SOLER et al., 2016; FELICIANO et al., 2017; THEEK et al., 2017), e por sua vez podem desencadear novos estímulos para formação, remodelamento e adaptação dos vasos dos neoplamas (NAGY et al., 2010; CLEGG & GABHANN., 2015).

A IL-8 é uma citocina indicada como reguladora do ambiente do neoplasma (YUAN et al., 2005; LEE et al., 2012; RAPOSO et al., 2015), visto que sua maior expressão já foi associada a células cancerosas (LIN et al., 2004; WAUGH & WILSON, 2008; ZUCCARI et al., 2011), a inflamação (SHAHZAD et al., 2010; MOHAMED et al., 2013; DIRKX et al., 2014) e a hipóxia (ANGELO & KURZROCK, 2007; GILKES & SEMENZA et al., 2013; SILVESTRE et al., 2013). Em nosso estudo, foi evidenciada a correlação da ecotextura heterogênea do neoplasma maligno e a mensuração sérica da IL-8, divergindo dos achados de outros estudos sorológicos, que não verificaram diferença nos estádios oncológicos iniciais (GELALETI et al., 2012; ANDRÉS et al., 2013; DERIN et al., 2007; MA et al., 2017; BENOY et al., 2004). Desta forma, a dosagem sérica da IL-8 nos neoplasmas malignos com ecotextura heterogênea, parece ser interessante na caracterização do neoplasma, visto que pode identificar lesões com potencial metastático local e distânte, assim como nos casos com estádio avançado e pior prognóstico, caracterizadas pelo aumento sérico desse mediador (BENOY et al., 2004; DERIN et al., 2007; MA et al., 2017).

Os índices Doppler velocimétricos (Vfl e IR) apresentaram relação com o VEGF, que pode ser secretado em maior quantidade por células cancerosas (NAGY et al., 2010), e tem maior efeito sobre células endoteliais (KERBEL, 2008). O VEGF está relacionado a várias etapas da vascularização tumoral (QIU et al., 2008; SHIVAKUMAR et al., 2009; SAPONARO et al., 2013), e a maior agressividade do neoplasma (DURANYILDIZ et al., 2008; KATO et al., 2007; SHIVAKUMAR et al., 2009). Assim, os achados relacionados ao aumento de Vfl e do IR dos vasos no neoplasma podem ser associados ao incremento do VEGF e sugerir a necessidade da terapia adjuvante nos estádios oncológicos I, II e III, devido a possível atividade angiogênica, que é fundamental na formação do foco metastático (ZUCCARI et al., 2016).

As variações morfológicas vasculares também podem alterar a dinâmica de fluxo e a perfusão no tumor (HOLOPAINEN et al., 2011; VIGER et al., 2014; LI et al., 2016) Entretanto, o método de caracterização da vascularização ao Doppler colorido, a partir da classificação em padrões não demonstrou diferenças nos níveis séricos de VEGF e de IL-8, entre o padrão vastular tipo mancha e o padrão vascular tipo rede. Para isso, talvez sejam necessárias técnicas

ultrassonográficas contrastadas para melhorar a precisão da avaliação do padrão vascular (STANZANI et al., 2014; YONGFENG et al., 2016; FELICIANO et al., 2017).

Em humanos, foi proposto a influência dos esteroides sexuais na expressão do VEGF, quando associado ao aumento tecidual do aporte vascular (HYDER, 2006; SANTOS et al., 2010; FAN et al., 2012). Desta forma, o VEGF produzido pode sofrer influência da atividade ovariana (FAN et al., 2012; HYDER, 2006; SANTOS et al., 2010). Em nossos achados, não houve diferença no nível sérico do E2 entre os grupos e, com isso, podemos sugerir a ausência da interferência estrogênica na mensuração sérica do VEGF, o que fortaleceu os achados da influência do fluxo sobre as células dos vassos no neoplasma (SILVESTRE et al., 2013).

As mamas mais acometidas foram as abdominais e inguinais. Fato que pode estar associado aos achados significativos hemodinâmicos na AECa, uma vez que, é o principal vaso de irrigação das glândulas mamárias abdominais e inguinais (SLEECKX et al., 2011). As Vfl acompanharam a demanda de irrigação ao maior número de lesão, sendo que, na ausência de lesão, as velocidades foram menores enquanto que, na presença de dois ou três nódulos ou massas, foram maiores, possivelmente em decorrência da maior demanda tecidual (SILVESTRE et al., 2013; LOGSDON et al., 2014; STANZANI et al., 2014CLEGG & MAC GABHANN, 2015; GOMPPER & FEDOSOV, 2016). No entanto, o reflexo do incremento da velocidade do fluxo devido ao maior número de neoplasmas não foi observado no IR, visto que ele não diferiu entre uma, duas e três lesões, demonstrando que o IR não está relacionado a quantidade de tecido a ser irrigado (Clegg and Mac Gabhann, 2015. Os achados podem ser justificados devido as características teciduais, como verificado a partir da ecotextura.

Os vasos do neoplasma (AUGUSTE et al., 2005; NAGY et al., 2010; STEFANINI et al., 2012; LOGSDON et al., 2014; CLEGG & MAC GABHANN, 2015) com apresentação de fluxo interno e periférico (SLEECKX et al., 2014) possibilitaram confrontar as variações na dinâmica de fluxo das artérias epigástricas e obter informações a respeito da vascularização formada, o que fortaleceu os achados hemodinâmicos nos neoplasmas mamários malignos (HUANG et al., 2013; DAVOUDI et al., 2014).

A baixa complacência tecidual, também já foi relacionada ao grau histológico (Del Cura et al., 2005; Zhou et al., 2013) e em nosso estudo foi verificada nos CM categorizados em grau I, II e não graduados, através do aumento do esforço de cisalhamento e da tensão circunferencial nas epigástricas a partir das Vfl e do IR.

6 CONCLUSÃO

O presente estudo apresenta uma importante aplicação da ecografia na oncologia veterinária, demonstrando o impacto hemodinâmico nas artérias epigástricas superficiais cranial e caudal ao Doppler ultrassonográfico no neoplasma mamário canino maligno. Diante dos resultados, sugere-se a avaliação dessas artérias, que irrigam a cadeia mamária acometida, juntamente com fatores associados a agressividade já relacionados na literatura, como ecotextura, hemodinâmica vascular do neoplasma, expressão sérica do fator de crescimento endotelial vascular e da interleucina-8. A partir desses, a ecografia é um exame não invasivo, de fácil acesso e que pode sugerir a necessidade de expandir o tratamento oncológico no pós-cirúrgico, nos estádios iniciais do neoplasma mamário canino.

REFERÊNCIAS

ANGELO, L. S.; KURZROCK, R. Vascular endothelial growth factor and its relationship to inflammatory mediators. **Clinical Cancer Research**, v. 13, n. 10, p. 2825–2830, 2007.

AUGUSTE, P. et al. Molecular mechanisms of tumor vascularization. **Critical Reviews in Oncology/Hematology**, v. 54, n. 1, p. 53–61, 2005.

BENOY, I. H. et al. Increased serum interleukin-8 in patients with early and metastatic breast cancer correlates with early dissemination and survival. **Clinical Cancer Research**, v. 10, n. 21, p. 7157–7162, 2004.

CANDELARIA, R. P. et al. Breast Ultrasound: Current Concepts. **Seminars in Ultrasound, CT and MRI**, v. 34, n. 3, p. 213–225, 2013.

CARMELIET, P. Mechanisms of angiogenesis and arteriogenesis. **Nature Medicine**, v. 6, n. 4, p. 389–395, 2000.

CARMELIET, P.; JAIN, R. K. Molecular mechanisms and clinical applications of angiogenesis. **Nature**, v. 473, n. 7347, p. 298–307, 2011.

CARVALHO, F. C. Ultrassonografia Doppler de linfonodos. In: CARVALHO, F. C., ed. **Ultrassonografia Doppler em pequenos animais**. 1. ed. São Paulo: Roca, p. 178-183, 2009.

CARVALHO, F. C. Ultrassonografia Duplex Doppler vascular: Aspectos Gerais. In: CARVALHO, F. C., ed. **Ultrassonografia Doppler em pequenos animais**. 1. ed. São Paulo: Roca, p. 87-97, 2009.

CASSALI, G. D. et al. Consensus for the diagnosis, prognosis and treatment of canine mammary tumors. **Brazilian Journal of Veterinary Pathology**, v. 4, n. 2, p. 153–180, 2011.

CLEGG, L. E.; MAC GABHANN, F. Systems biology of the microvasculature. **Integr. Biol.**, v. 7, n. 5, p. 498–512, 2015.

CLEMENTE, M. et al. Histological, immunohistological, and ultrastructural description of vasculogenic mimicry in canine mammary cancer. **Veterinary Pathology**, v. 47, n. 2, p. 265–274, 2010.

CLEMENTE, M.; PÉREZ-ALENZA, M. D.; PEÑA, L. Metastasis of canine inflammatory versus non-inflammatory mammary tumours. **Journal of Comparative Pathology**, v. 143, n. 2–3, p. 157–163, 2010.

DAVOUDI, Y. et al. The role of doppler sonography in distinguishing malignant from benign breast lesions. **Journal of Medical Ultrasound**, v. 22, n. 2, p. 92–95, 2014.

DE ANDRÉS, P. J. et al. Increased levels of interleukins 8 and 10 as findings of canine inflammatory mammary cancer. **Veterinary Immunology and Immunopathology**, v. 152, n. 3–4, p. 245–251, 2013.

DEL CURA, J. L. et al. The use of unenhanced doppler sonography in the evaluation of solid

breast lesions. **American Journal of Roentgenology**, v. 184, n. 6, p. 1788–1794, 2005.

DERIN, D. et al. Serum IL-8 and IL-12 levels in breast cancer. **Medical Oncology**, v. 24, n. 2, p. 163–168, 2007.

DIESSLER, M. E. et al. Canine mammary carcinomas: influence of histological grade, vascular invasion, proliferation, microvessel density and VEGFR2 expression on lymph node status and survival time. **Veterinary and Comparative Oncology**, v. 15, n. 2, p. 450–461, 2017.

DIRKX, A. E. M. et al. Monocyte/macrophage infiltration in tumors: modulators of angiogenesis. **Journal of Leukocyte Biology**, v. 80, n. 6, p. 1183–1196, 2006.

DURANYILDIZ, D. et al. Serum levels of angiogenic factors in early breast cancer remain close to normal. **Breast**, v. 18, n. 1, p. 26–29, 2009.

FELICIANO, M. A. R. et al. ARFI elastography as a complementary diagnostic method for mammary neoplasia in female dogs - preliminary results. **Journal of Small Animal Practice**, v. 55, n. 10, p. 504–508, 2014.

FELICIANO, M. A. R. et al. Ultrasonography methods for predicting malignancy in canine mammary tumors. **PLoS ONE**, v. 12, n. 5, p. 1–15, 2017.

FELICIANO, M. A. R.; VICENTE, W. R. R.; SILVA, M. A. M. Conventional and Doppler ultrasound for the differentiation of benign and malignant canine mammary tumours. **Journal of Small Animal Practice**, v. 53, n. 6, p. 332–337, 2012.

FERREIRA, E. et al. The relationship between tumour size and expression of prognostic markers in benign and malignant canine mammary tumours. **Veterinary and Comparative Oncology**, v. 7, n. 4, p. 230–235, 2009.

GELALETI, G. B. et al. Interleukin-8 as a prognostic serum marker in canine mammary gland neoplasias. **Veterinary Immunology and Immunopathology**, v. 146, n. 2, p. 106–112, 2012.

GILKES, D. M.; SEMENZA, G. L. Role of hypoxia-inducible factors in breast cancer metastasis. **Future Oncology**, v. 9, n. 11, p. 1623–1636, 2013.

GOLDSCHMIDT MH, PEÑA L, RASOTTO R, ZAPPULLI V. Classification and grading of canine mammary tumors. **Vet Pathol**, v. 48, n. 1, p. 117-131, 2011.

GOKALP, G.; TOPAL, U.; KIZILKAYA, E. Power Doppler sonography: Anything to add to BI-RADS US in solid breast masses? **European Journal of Radiology**, v. 70, n. 1, p. 77–85, 2009.

GOMPPER, G.; FEDOSOV, D. A. Modeling microcirculatory blood flow: Current state and future perspectives. **Wiley Interdisciplinary Reviews: Systems Biology and Medicine**, v. 8, n. 2, p. 157–168, 2016.

HANAHAN, D.; FOLKMAN, J. Patterns and emerging mechanisms of the angiogenic switch during tumorigenesis. **Cell**, v. 86, n. 3, p. 353–364, 1996.

HANAHAN, D.; WEINBERG, R. A. Hallmarks of cancer: The next generation. **Cell**, v. 144, n. 5, p. 646–674, 2011.

HOFFMANN, B.; SCHULER, G. Receptor blockers - General aspects with respect to their use in domestic animal reproduction. **Animal Reproduction Science**, v. 60–61, p. 295–312, 2000.

HOLOPAINEN, T. et al. Perspectives on lymphangiogenesis and angiogenesis in cancer. **Journal of Surgical Oncology**, v. 103, n. 6, p. 484–488, 2011.

HUANG, Y.-H. et al. Diagnosis of Solid Breast Tumors Using Vessel Analysis in Three-Dimensional Power Doppler Ultrasound Images. **Journal of Digital Imaging**, v. 26, n. 4, p. 731–739, 2013.

KAREVA, I. Escape from tumor dormancy and time to angiogenic switch as mitigated by tumor-induced stimulation of stroma. **Journal of Theoretical Biology**, v. 395, p. 11–22, 2016.

KATO, Y. et al. Clinical significance of circulating vascular endothelial growth factor in dogs with mammary gland tumors. **The Journal of veterinary medical science / the Japanese Society of Veterinary Science**, v. 69, p. 77–80, 2007.

KERBEL, R. S. Tumor Angiogenesis. **Health (San Francisco)**, p. 2039–2049, 2008.

KIM, E. et al. Multiscale imaging and computational modeling of blood flow in the tumor vasculature. **Annals of Biomedical Engineering**, v. 40, n. 11, p. 2425–2441, 2012.

KWAK, J. Y. et al. Power Doppler sonography: evaluation of solid breast lesions and correlation with lymph node metastasis. **Clinical Imaging**, v. 32, n. 3, p. 167–171, 2008.

LEE, G. S. et al. Blood flow shapes intravascular pillar geometry in the chick chorioallantoic membrane. **Journal of Angiogenesis Research**, v. 2, n. 1, p. 1–9, 2010.

LEE, W. J. et al. Breast cancer vascularity: Color Doppler sonography and histopathology study. **Breast Cancer Research and Treatment**, v. 37, n. 3, p. 291–298, 1996.

LEE, Y. S. et al. Interleukin-8 and its receptor CXCR2 in the tumour microenvironment promote colon cancer growth, progression and metastasis. **British Journal of Cancer**, v. 106, n. 11, p. 1833–1841, 2012.

LI, S. et al. The hypoxia-related signaling pathways of vasculogenic mimicry in tumor treatment. **Biomedicine and Pharmacotherapy**, v. 80, p. 127–135, 2016.

LIN, Y. et al. Identification of interleukin-8 as estrogen receptor-regulated factor involved in breast cancer invasion and angiogenesis by protein arrays. **International Journal of Cancer**, v. 109, n. 4, p. 507–515, 2004.

LOGSDON, E. A. et al. A systems biology view of blood vessel growth and remodelling. **Journal of Cellular and Molecular Medicine**, v. 18, n. 8, p. 1491–1508, 2014.

LOH, Z. H. K. et al. Ultrasonographic characteristics of soft tissue tumours in dogs. **Australian Veterinary Journal**, v. 87, n. 8, p. 323–329, 2009.

MA, Y. et al. IL-6, IL-8 and TNF-α levels correlate with disease stage in breast cancer patients. **Advances in Clinical and Experimental Medicine**, v. 26, n. 3, p. 421–426, 2017.

MILLANTA, F. et al. Expression of Vascular Endothelial Growth Factor in Canine Inflammatory and Non-inflammatory Mammary Carcinoma. **Journal of Comparative Pathology**, v. 142, n. 1, p. 36–42, 2010.

MOHAMED, M. M. et al. Inflammatory breast cancer: New factors contribute to disease etiology: A review. **Journal of Advanced Research**, v. 5, n. 5, p. 525–536, 2014.

MORI, N. et al. Quantitative Analysis of Contrast-Enhanced Ultrasound Imaging in Invasive Breast Cancer: A Novel Technique to Obtain Histopathologic Information of Microvessel Density. **Ultrasound in Medicine and Biology**, v. 43, n. 3, p. 607–614, 2017.

NAGY, J. A. et al. Heterogeneity of the tumor vasculature. **Seminars in Thrombosis and Hemostasis**, v. 36, n. 3, p. 321–331, 2010.

OK-CHAO, T. C. et al. Color Doppler ultrasound in benign and malignant breast tumors. **Breast Cancer Research and Treatment**, v. 57, n. 2, p. 193–199, 1999.

PEREZ-RIVAS, L. G. et al. Serum protein levels following surgery in breast cancer patients: A protein microarray approach. **International Journal of Oncology**, v. 41, n. 6, p. 2200–2206, 2012.

PODAR, K. et al. Targeting the tumor microenvironment: Focus on angiogenesis. **Journal of Oncology**, v. 2012, 2012.

QIU, C. W. et al. Expression and significance of PTEN and VEGF in canine mammary gland tumours. **Veterinary Research Communications**, v. 32, n. 6, p. 463–472, 2008.

QUEIROGA, F. L. et al. Canine mammary tumours as a model to study human breast cancer: most recent findings. **In vivo (Athens, Greece)**, v. 25, n. 3, p. 455–465, 2011.

RAPOSO, T. P. et al. Inflammation and cancer: Till death tears them apart. **Veterinary Journal**, v. 205, n. 2, p. 161–174, 2015.

RESTUCCI, B. Evaluation of Angiogenesis in Canine Mammary Tumors by Quantitative Platelet Endothelial Cell Adhesion Molecule Immunohistochemistry. **Veterinary Pathology**, v. 37, n. 4, p. 297–301, 2000.

SANTOS, A. A. et al. Identification of prognostic factors in canine mammary malignant tumours : a multivariable survival study. p. 1–11, 2013.

SANTOS, A. A. F. et al. Immunohistochemical Expression of Vascular Endothelial Growth Factor in Canine Mammary Tumours. **Journal of Comparative Pathology**, v. 143, n. 4, p. 268–275, 2010.

SANTOS, A. A.; MATOS, A. J. F. Advances in the understanding of the clinically relevant genetic pathways and molecular aspects of canine mammary tumours. Part 2: Invasion,

angiogenesis, metastasis and therapy. **Veterinary Journal**, v. 205, n. 2, p. 144–153, 2015.

SAPONARO, C. et al. VEGF, HIF-1α Expression and MVD as an Angiogenic Network in Familial Breast Cancer. **PLoS ONE**, v. 8, n. 1, p. 1–8, 2013.

SHAHZAD, A. et al. Interleukin 8 (IL-8) - a universal biomarker? **International Archives of Medicine**, v. 3, n. 1, p. 11, 2010.

SHIVAKUMAR, S. et al. Evaluation of serum vascular endothelial growth factor (VEGF) and microvessel density (MVD) as prognostic indicators in carcinoma breast. **Journal of Cancer Research and Clinical Oncology**, v. 135, n. 4, p. 627–636, 2009.

SILVESTRE, J.-S.; SMADJA, D. M.; LEVY, B. I. Postischemic Revascularization: From Cellular and Molecular Mechanisms to Clinical Applications. **Physiological Reviews**, v. 93, n. 4, p. 1743–1802, 2013.

SLEECKX, N. et al. Canine Mammary Tumours, an Overview. **Reproduction in Domestic Animals**, v. 46, n. 6, p. 1112–1131, 2011.

SLEECKX, N. et al. Angiogenesis in Canine Mammary Tumours: A Morphometric and Prognostic Study. **Journal of Comparative Pathology**, v. 150, n. 2–3, p. 175–183, 2014.

SOLER, M. et al. Comparison between ultrasonographic findings of benign and malignant canine mammary gland tumours using B-mode, colour Doppler, power Doppler and spectral Doppler. **Research in Veterinary Science**, v. 107, p. 141–146, 2016.

SORENMO, K. U. et al. Development, anatomy, histology, lymphatic drainage, clinical features, and cell differentiation markers of canine mammary gland neoplasms. **Veterinary Pathology**, v. 48, n. 1, p. 85–97, 2011.

STAMATELOS, S. K. et al. A bioimage informatics based reconstruction of breast tumor microvasculature with computational blood flow predictions. **Microvascular Research**, v. 91, p. 8–21, 2014.

STANZANI, D. et al. Can Doppler or contrast-enhanced ultrasound analysis add diagnostically important information about the nature of breast lesions? **Clinics**, v. 69, n. 2, p. 87–92, 2014.

STEFANINI, M. O. et al. Computational models of VEGF-associated angiogenic processes in cancer. **Mathematical Medicine and Biology**, v. 29, n. 1, p. 85–94, 2012.

THEEK, B. et al. Automated generation of reliable blood velocity parameter maps from contrast-enhanced ultrasound data. **Contrast Media and Molecular Imaging**, v. 2017, 2017.

VIGER, L. et al. A cancer model for the angiogenic switch. **Journal of Theoretical Biology**, v. 360, p. 21–33, 2014.

WAUGH, D. J. J.; WILSON, C. The interleukin-8 pathway in cancer. **Clinical Cancer Research**, v. 14, n. 21, p. 6735–6741, 2008.

YONGFENG, Z. et al. Application of a Novel Microvascular Imaging Technique in Breast

Lesion Evaluation. **Ultrasound in Medicine and Biology**, v. 42, n. 9, p. 2097–2105, 2016.

YUAN, A. et al. The role of interleukin-8 in cancer cells and microenvironment interaction. **Frontiers in bioscience : a journal and virtual library**, v. 10, n. 5, p. 853–65, 2005.

ZHAO, J. et al. Correlation between serum vascular endothelial growth factor and endostatin levels in patients with breast cancer. **Cancer Letters**, v. 204, n. 1, p. 87–95, 2004.

ZHOU, J. et al. Role of Acoustic Shear Wave Velocity Measurement in Characterization of Breast Lesions. **J. Ultrasound Med.**, v. 32, n. 2, p. 285–294, 2013.

ZUCCARI, D. A P. C. et al. Interleukin-8 expression associated with canine mammary tumors. **Genetics and molecular research : GMR**, v. 10, n. 3, p. 1522–32, 2011.